

Article

# High-Order Approximation to Generalized Caputo Derivatives and Generalized Fractional Advection–Diffusion Equations

Sarita Kumari <sup>1,\*</sup>, Rajesh K. Pandey <sup>1,\*</sup> and Ravi P. Agarwal <sup>2,\*</sup>

<sup>1</sup> Department of Mathematical Sciences, Indian Institute of Technology (BHU) Varanasi, Varanasi 221005, Uttar Pradesh, India

<sup>2</sup> Department of Mathematics, Texas A & M University-Kingsville, Kingsville, TX 77553, USA

\* Correspondence: rkpandey.mat@iitbhu.ac.in (R.K.P.); ravi.agarwal@tamuk.edu (R.P.A.)

**Abstract:** In this article, a high-order time-stepping scheme based on the cubic interpolation formula is considered to approximate the generalized Caputo fractional derivative (GCFD). Convergence order for this scheme is  $(4 - \alpha)$ , where  $\alpha$  ( $0 < \alpha < 1$ ) is the order of the GCFD. The local truncation error is also provided. Then, we adopt the developed scheme to establish a difference scheme for the solution of the generalized fractional advection–diffusion equation with Dirichlet boundary conditions. Furthermore, we discuss the stability and convergence of the difference scheme. Numerical examples are presented to examine the theoretical claims. The convergence order of the difference scheme is analyzed numerically, which is  $(4 - \alpha)$  in time and second-order in space.

**Keywords:** generalizedCaputo fractional derivative; generalized fractional advection–diffusion equation; difference scheme; stability; numerical solutions

**MSC:** 26A33; 35R11; 35A35; 65M06



**Citation:** Kumari, S.; Pandey, R.K.; Agarwal, R.P. High-Order Approximation to Generalized Caputo Derivatives and Generalized Fractional Advection–Diffusion Equations. *Mathematics* **2023**, *11*, 1200. <https://doi.org/10.3390/math11051200>

Academic Editors: Andrey Zahariev and Hristo Kiskinov

Received: 21 December 2022

Revised: 19 February 2023

Accepted: 23 February 2023

Published: 28 February 2023



**Copyright:** © 2023 by the authors. Licensee MDPI, Basel, Switzerland. This article is an open access article distributed under the terms and conditions of the Creative Commons Attribution (CC BY) license (<https://creativecommons.org/licenses/by/4.0/>).

## 1. Introduction

This work includes the numerical solution of the following generalized fractional advection–diffusion equation,

$$\begin{cases} {}_0^C \mathcal{D}_{t;[\zeta(t),\omega(t)]}^\alpha U(x,t) = D \frac{\partial^2 U(x,t)}{\partial x^2} - A \frac{\partial U(x,t)}{\partial x} + g(x,t), & x \in \Omega, \quad t \in (0,T], \\ U(x,0) = U_0(x), & x \in \bar{\Omega} = \Omega \cup \partial\Omega, \\ U(0,t) = \rho_1(t), \quad U(a,t) = \rho_2(t), & t \in (0,T], \end{cases} \quad (1)$$

where  $\Omega = (0, a)$  is a bounded domain with boundary  $\partial\Omega$  and the notation  ${}_0^C \mathcal{D}_{t;[\zeta(t),\omega(t)]}^\alpha$  denotes the GCFD (defined in [1] and related references therein) with respect to  $t$  of order  $\alpha$ :

$${}_0^C \mathcal{D}_{t;[\zeta(t),\omega(t)]}^\alpha U(t) = \frac{[\omega(t)]^{-1}}{\Gamma(1-\alpha)} \int_0^t \frac{[\omega(s)U(s)]'}{[\zeta(t) - \zeta(s)]^\alpha} ds, \quad 0 < \alpha < 1, \quad (2)$$

where  $\partial_s = \frac{\partial}{\partial s}$ , parameter  $D > 0$  is the diffusivity,  $A > 0$  is the advection constant and  $U$  is the solute concentration;  $g$ ,  $U_0$ ,  $\rho_1$  and  $\rho_2$  are continuous functions on their respective domains with  $U_0(0) = \rho_1(0)$  and  $U_0(a) = \rho_2(0)$ . Here scale and weight are sufficiently regular functions and our model (1) reduces to the diffusion problem when  $A = 0$ . The advection–diffusion equation is basically a transport problem that transports a passive scalar quantity in a fluid flow. Due to diffusion and advection, this model represents the physical phenomenon of species concentration for mass transfer and temperature in heat transfer; for more details, refer to [2–6], and [7–11] for further history and significance of the advection–diffusion equation in physics, chemistry and biology.

The most used fractional derivatives in the problem formulation are the Riemann–Liouville and the Caputo derivatives [12]. In the year 2012, the generalizations of fractional integrals and derivatives were discussed by Agrawal [1]. Two functions, scale  $\zeta(t)$  and weight  $\omega(t)$  in one parameter, appear in the definition of the generalized fractional derivative of a function  $\mathcal{V}(t)$ . If  $\omega(t) = 1$  and  $\zeta(t) = t$  then the generalized fractional derivative reduces to the Riemann–Liouville (R-L) and the Caputo derivative; whereas if  $\omega(t) = 1$ ,  $\zeta(t) = \ln(t)$ , and  $\omega(t) = t^{\sigma\eta}$ ,  $\zeta(t) = t^\sigma$  then it will convert to Hadamard [13], and modified Erdélyi–Kober fractional derivatives, respectively. The authors of [14] studied the generalized form of R-L and the Hadamard fractional integrals, which is a special case of the Erdélyi–Kober generalized fractional derivative, and some properties of this operator. Atangana and Baleanu [15] discussed a new fractional derivative with a non-singular kernel and used this derivative in the formation of a fractional heat transfer model. Therefore, we obtain different types of fractional derivatives for different choices of weight and scale functions. In the generalized derivative, the scale function  $\zeta(t)$  manages the considered time domain; it can stretch or contract accordingly to capture the phenomena accurately over the desired time range. The weight function  $\omega(t)$  allows the events to be estimated differently at different times.

Over the last decade, many numerical methods were investigated to approximate the Caputo fractional derivative. For example, Mustapha [16] presented an  $L1$  approximation formula to solve a fractional reaction–diffusion equation and second-order error bound discussed on non-uniform time meshes. Alikhanov [17] constructed an  $L2 - 1_\sigma$  formula to approximate the Caputo fractional time derivative and then used this derived scheme in solving the time fractional diffusion equation with variable coefficients. Abu Arqub [18] considered reproducing a kernel algorithm for approximate solution of the nonlinear time-fractional PDEs with initial and Robin boundary conditions. Li and Yan [19] discussed the idea of [20] (i.e.,  $L2$  approximation formula for time discretization), and also derived a new time discretization method with accuracy order  $\mathcal{O}(\tau^{3-\alpha})$  and finite element method for spatial discretization. Cao et al. [21] presented a high-order approximation formula based on the cubic interpolation to approximate the Caputo derivative for the time fractional advection–diffusion equation. Xu and Agrawal [22] used the finite difference method (FDM) to approximate the GCFD for solving the generalized fractional Burgers equation. Kumar et al. [23] presented  $L1$  and  $L2$  methods to approximate the generalized time fractional derivative which are defined as follows, respectively

$${}_0^C \mathcal{D}_{t;[\zeta(t),\omega(t)]}^\alpha \mathcal{V}(t)|_{t=t_n} = \frac{[\omega(t)]^{-1}}{\Gamma(1-\alpha)} \sum_{l=1}^n \left( \frac{\omega_l \mathcal{V}_l - \omega_{l-1} \mathcal{V}_{l-1}}{\zeta_l - \zeta_{l-1}} \right) \int_{t_{l-1}}^{t_l} [\zeta(t) - \zeta(s)]^{-\alpha} (\partial_s \zeta(s)) ds + r_1^n, \tag{3}$$

$${}_0^C \mathcal{D}_{t;[\zeta(t),\omega(t)]}^\alpha \mathcal{V}(t)|_{t=t_n} = \frac{[\omega(t)]^{-1}}{\Gamma(1-\alpha)} \sum_{l=1}^n \int_{t_{l-1}}^{t_l} [\zeta(t) - \zeta(s)]^{-\alpha} \partial_s (\Pi_l \omega(s) \mathcal{V}(s)) ds + r_2^n, \tag{4}$$

where,

$$\Pi_l'(\omega(t)\mathcal{V}(t)) = \zeta'(t) \left\{ \left[ \frac{2\zeta(t) - \zeta_l - \zeta_{l-1}}{(\zeta_{l-2} - \zeta_{l-1})(\zeta_{l-2} - \zeta_{l-1})} \right] \omega_{l-2} \mathcal{V}_{l-2} + \left[ \frac{2\zeta(t) - \zeta_l - \zeta_{l-2}}{(\zeta_{l-1} - \zeta_{l-2})(\zeta_{l-1} - \zeta_l)} \right] \omega_{l-1} \mathcal{V}_{l-1} + \left[ \frac{2\zeta(t) - \zeta_{l-1} - \zeta_{l-2}}{(\zeta_l - \zeta_{l-2})(\zeta_l - \zeta_{l-1})} \right] \omega_l \mathcal{V}_l \right\},$$

where the domain  $[0, T]$  was discretized into  $n$  equal subintervals, i.e.,  $0 = t_0 < t_1 < \dots < t_N = T$  with step-size  $\tau = \frac{T}{N}$ , and errors  $r_1^n = \mathcal{O}(\tau^{2-\alpha})$ ,  $r_2^n = \mathcal{O}(\tau^{3-\alpha})$  were shown in [23]. In this work, we discuss the numerical scheme for GCFD with convergence rate  $(4 - \alpha)$ ; for this accuracy we have to assume that  $\mathcal{V}'(t_0) = 0$ ,  $\mathcal{V}''(t_0) = 0$ ,  $\mathcal{V}'''(t_0) = 0$ . This idea is discussed in [21] for Caputo derivative approximation, but the error bound was discussed directly.

Due to the non-local property of the fractional derivatives, the numerical solution of the fractional partial differential equations is a very difficult task [24]. Several authors have presented some precise and efficient numerical methods for the fractional advection–diffusion equation. For examples, Zheng et al. [25] used the finite element method (FEM) for space fractional advection–diffusion equation. Mardani et al. [26] discussed meshless moving least square method for solving the time-fractional advection–diffusion equation with variable coefficients. Cao et al. [21] proposed the higher-order approximation of the Caputo derivatives and further applied it in solving the fractional advection–diffusion equation. They used the Lagrange interpolation method to discretize the time derivative and second-order central difference for the spatial derivatives. Li and Cai [27] considered a three-step process for the Caputo fractional derivative approximation; the first two steps include the shifted Lubich formula derivation for infinite interval then for finite interval, and after that it is generalized to the Caputo derivative. Yadav et al. [28] discussed the Taylor expansion for the approximation of the generalized time-fractional derivative to solve the generalized fractional advection–diffusion equation. Tian et al. [29] presented a polynomial spectral collocation method for the space fractional advection–diffusion equation. In [30], the authors developed explicit and implicit Euler approximations to solve a variable-order fractional advection–diffusion equation on a finite domain. Singh et al. [31] investigated the numerical approximation of the Caputo–Prabhakar derivative and then used this approximation to solve the fractional advection–diffusion equation. Kannan et al. [32] used a variant of the local discontinuous Galerkin (LDG2) flux formulation to discuss the high accuracy of the 1D and 2D diffusion equations. In [33], the authors discussed three approaches, penalty approach, BR2 (Bassi and Rebay) method and LDG method, to study the 2D diffusion equation.

### 1.1. Motivation and Literature Review for Approximation of the GCFD

Up to now, there are only limited works available in the literature to approximate the GCFD. These works include the finite difference method,  $L1$ -method,  $L1 - 2$ -method and collocation method used to approximate GCFD. In this article, we present the approximation of the GCFD based on cubic interpolation polynomials (say  $L1 - 2 - 3$ -method).

- Xu and Agrawal [22] considered the FDM for approximation of the GCFD for the generalized fractional Burgers equation.
- Kumar et al. [34] presented a numerical scheme for the generalized fractional telegraph equation in time.
- Cao et al. [35] worked on the generalized time-fractional Kdv equation. They used the collocation method which is constructed using Jacobi–Gauss–Lobatto (JGL) nodes.
- Xu et al. [36] considered the FDM to approximate the GCFD of order  $0 < \alpha < 1$  and discussed the analytical and numerical solutions of the generalized fractional diffusion equation.
- In [37], the authors used the generalized weighted and shifted Grünwald–Letnikov difference operator to approximate the GCFD and then adopt it to solve the generalized fractional diffusion equation.
- Yadav et al. [28] discussed the Taylor expansion and finite difference approach to approximate the GCFD and then presented the numerical solution of the generalized fractional advection–diffusion equation.
- Sultana et al. [38] presented a numerical scheme based on non-uniform meshes for solution of the generalized time-fractional telegraph equation using quadratic interpolation and compact finite difference approximations for temporal and spatial directions respectively.

Motivated by all these works, the main focus of this paper is to present a much higher-order numerical scheme to approximate the GCFD, and also establish the error analysis in both time and space discretization. To the best of our knowledge, no work has been done yet for a third-order error bound of cubic interpolation formula to approximate the GCFD.

1.2. The Main Contributions of This Work Are as Follows

(1) We extend the approximation method of Cao et al. [21] for approximating the GCFD and obtain the convergence order  $(4 - \alpha)$ . Further, we show that the obtained scheme reduces to the approximation scheme discussed by Cao et al. [21] for choice of the scale and the weight functions as  $\zeta(t) = t$  and  $\omega(t) = 1$ .

(2) We establish the full error analysis of the presented higher-order numerical scheme for the generalized time fractional derivative by using the Lagrange interpolation formula.

(3) We introduce some numerical results for different choices of scale and weight functions for the high-order time discretization scheme with convergence order  $\mathcal{O}(\tau^{4-\alpha})$  for all  $\alpha \in (0, 1)$  which achieves higher accuracy than the numerical methods developed in Gao et al. [39] for  $\zeta(t) = t$  and  $\omega(t) = 1$ .

The remaining sections of the paper are arranged as follows: In Section 2, we discuss the  $(4 - \alpha)$ -th order scheme to approximate the GCFD of order  $\alpha$  of the function  $\mathcal{V}$ . In Section 3, a higher-order difference scheme to solve the generalized fractional advection–diffusion equation is presented. Stability and convergence analysis are also discussed in this section. We present three numerical examples which illustrate the error and convergence order of our established numerical scheme in Section 4. Finally, Section 5 concludes with some remarks.

2. Numerical Scheme for the Generalized Caputo Fractional Derivative

Motivated by the research carried out in [21,23], this section is devoted to presenting a high-order approximation formula for the generalized Caputo-type fractional derivative using cubic interpolation polynomials.

Suppose that  $\mathcal{V}(t) \in C^4[0, T]$  and grid points  $0 = t_0 < t_1 < \dots < t_N = T$  with step length  $\tau = t_n - t_{n-1}$  for  $1 \leq n \leq N$ . For simplicity, we use  $g(s) = \omega(s)\mathcal{V}(s)$ ,  $\mathcal{V}(t_l) = \mathcal{V}_l$ ,  $\omega(t_l) = \omega_l$  and  $\zeta(t_l) = \zeta_l$ . The generalized Caputo fractional derivative of order  $\alpha$  of the function  $\mathcal{V}(t)$  at grid point  $t_n$  is given by,

$${}_0^C \mathcal{D}_{t;[\zeta(t),\omega(t)]}^\alpha \mathcal{V}_n = \frac{[\omega_n]^{-1}}{\Gamma(1-\alpha)} \sum_{l=1}^n \int_{t_{l-1}}^{t_l} \frac{g'(s)}{[\zeta(t_n) - \zeta(s)]^\alpha} ds. \tag{5}$$

On the first interval  $[0, t_1]$  of the domain, we use continuous linear polynomial  $\Pi_1 g(t)$  to approximate the function  $g(t) (= \omega(t)\mathcal{V}(t))$ . Let  $g(t_l) = g_l$  and the difference operator  $\nabla_\tau g_l = g_l - g_{l-1}$  for  $l \geq 1$ . Then, we have

$$(\Pi_1 g(t))' = \frac{(g_1 - g_0)}{\tau} = \frac{(\nabla_\tau g_1)}{\tau}.$$

Thus, Equation (5) yields,

$$\begin{aligned} \frac{[\omega_n]^{-1}}{\Gamma(1-\alpha)} \int_0^{t_1} [\zeta(t_n) - \zeta(s)]^{-\alpha} g'(s) ds &= \frac{[\omega_n]^{-1}}{\Gamma(1-\alpha)} \frac{(\nabla_\tau g_1)}{\tau} \int_0^{t_1} [\zeta(t_n) - \zeta(s)]^{-\alpha} ds + E_\tau^1 \\ &= a_{n-1}(\nabla_\tau g_1) + E_\tau^1, \end{aligned} \tag{6}$$

where  $E_\tau^1$  is the truncation error on the first interval and coefficients for this approximation are

$$a_{n-1} = \frac{[\omega_n]^{-1}}{\Gamma(2-\alpha)} \left\{ \frac{[\zeta(t_n) - \zeta(t_{l-1})]^{1-\alpha} - [\zeta(t_n) - \zeta(t_l)]^{1-\alpha}}{[\zeta(t_l) - \zeta(t_{l-1})]} \right\}.$$

Here, we denote notation  $\alpha_0^{(n)} = \frac{[\omega_n]^{-1}}{\Gamma(2-\alpha)}$ ,  $1 \leq n \leq N$ . Then

$$a_{n-l} = \alpha_0^{(n)} \left\{ \frac{[\zeta(t_n) - \zeta(t_{l-1})]^{1-\alpha} - [\zeta(t_n) - \zeta(t_l)]^{1-\alpha}}{[\zeta(t_l) - \zeta(t_{l-1})]} \right\}, \quad 1 \leq l \leq n. \tag{7}$$

**Remark 1.** If the scale function  $\zeta$  is a positive strictly increasing function on the domain  $[0, T]$ , then the following inequality holds

$$0 < [\zeta(t_n) - \zeta(t_l)]^{1-\alpha} - [\zeta(t_n) - \zeta(t_{l-1})]^{1-\alpha}, \quad 1 \leq l \leq n. \tag{8}$$

Since  $t_l > t_{l-1}$ , then it implies  $\zeta(t_l) > \zeta(t_{l-1})$  for  $1 \leq l \leq n$ , also  $(1 - \alpha) > 0$ .

**Remark 2.** To estimate  $a_{n-1}$ , suppose that

$$\Theta = [\zeta(t_n) - \zeta(s)] \Rightarrow d\Theta = -\zeta'(s) ds = -\left(\frac{\zeta(t_l) - \zeta(t_{l-1})}{\tau}\right) ds, \quad s \in (t_{l-1}, t_l),$$

therefore,

$$\int [\zeta(t_n) - \zeta(s)]^{-\alpha} ds = \frac{-\tau}{\zeta(t_l) - \zeta(t_{l-1})} \frac{[\zeta(t_n) - \zeta(s)]^{1-\alpha}}{(1-\alpha)}.$$

On the second interval  $[t_1, t_2]$ , we use the continuous quadratic polynomial  $\Pi_2g(t)$  to approximate the function  $g(t)$ , then we get

$$(\Pi_2g(t))' = \frac{(2t - t_0 - t_1)}{2\tau^2}g_2 - \frac{(2t - t_0 - t_2)}{\tau^2}g_1 + \frac{(2t - t_1 - t_2)}{2\tau^2}g_0.$$

Thus from Equation (5), we get,

$$\begin{aligned} \frac{[\omega_n]^{-1}}{\Gamma(1-\alpha)} \int_{t_1}^{t_2} [\zeta(t_n) - \zeta(s)]^{-\alpha} g'(s) ds &= \frac{[\omega_n]^{-1}}{\Gamma(1-\alpha)} \int_{t_1}^{t_2} [\zeta(t_n) - \zeta(s)]^{-\alpha} (\Pi_2g(s))' ds + E_\tau^2 \\ &= a_{n-2}(g_2 - g_1) + b_{n-2}(g_2 - 2g_1 + g_0) + E_\tau^2 \\ &= a_{n-2}(\nabla_\tau g_2) + b_{n-2}(\nabla_\tau^2 g_2) + E_\tau^2. \end{aligned} \tag{9}$$

Here, the truncation error on the second interval is  $E_\tau^2$ , and

$$\begin{aligned} b_{n-l} = \alpha_0^{(n)} \left\{ \frac{1}{(2-\alpha)} \left[ \frac{[\zeta(t_n) - \zeta(t_{l-1})]^{2-\alpha} - [\zeta(t_n) - \zeta(t_l)]^{2-\alpha}}{[\zeta(t_l) - \zeta(t_{l-1})]^2} \right] \right. \\ \left. - \frac{1}{2} \left[ \frac{[\zeta(t_n) - \zeta(t_{l-1})]^{1-\alpha} + [\zeta(t_n) - \zeta(t_l)]^{1-\alpha}}{[\zeta(t_l) - \zeta(t_{l-1})]} \right] \right\}, \quad 2 \leq l \leq n. \end{aligned} \tag{10}$$

On the other subdomains ( $l \geq 3$ ), we use the cubic interpolation polynomial  $\Pi_lg(t)$  to approximate the function  $g(t)$  using four points  $(t_{l-3}, g_{l-3}), (t_{l-2}, g_{l-2}), (t_{l-1}, g_{l-1}), (t_l, g_l)$ . As we know the cubic interpolation polynomial is defined as:

$$\Pi_lg(t) = \sum_{r=0}^3 g_{l-r} \prod_{s=0, s \neq r}^3 \left( \frac{t - t_{l-s}}{t_{l-r} - t_{l-s}} \right),$$

then we get,

$$\begin{aligned} (\Pi_lg(t))' &= g_{l-3} \frac{(t - t_{l-2})(t_l + t_{l-1} - 2t) + (t - t_{l-1})(t_l - t)}{6\tau^3} \\ &+ g_{l-2} \frac{(t - t_{l-3})(2t - t_{l-1} - t_l) + (t - t_l)(t - t_{l-1})}{2\tau^3} \\ &+ g_{l-1} \frac{(t - t_{l-2})(t_{l-3} + t_l - 2t) + (t - t_{l-3})(t_l - t)}{2\tau^3} \\ &+ g_l \frac{(t - t_{l-2})(2t - t_{l-3} - t_{l-1}) + (t - t_{l-1})(t - t_{l-3})}{6\tau^3}. \end{aligned}$$

Therefore, from Equation (5), we have,

$$\begin{aligned} & \frac{[\omega_n]^{-1}}{\Gamma(1-\alpha)} \sum_{l=3}^n \int_{t_{l-1}}^{t_l} [\zeta(t_n) - \zeta(s)]^{-\alpha} g'(s) ds \\ &= \frac{[\omega_n]^{-1}}{\Gamma(1-\alpha)} \sum_{l=3}^n \int_{t_{l-1}}^{t_l} [\zeta(t_n) - \zeta(s)]^{-\alpha} (\Pi_l g(s))' ds + E_\tau^n \\ &= \sum_{l=3}^n \left[ A_{1,n-l} g_l + A_{2,n-l} g_{l-1} + A_{3,n-l} g_{l-2} + A_{4,n-l} g_{l-3} \right] + E_\tau^n, \end{aligned} \tag{11}$$

where  $E_\tau^n$  ( $3 \leq n \leq N$ ) is the truncation error, and

$$\begin{aligned} A_{1,n-l} = \alpha_0^{(n)} & \left\{ \frac{1}{6} \left[ \frac{2[\zeta(t_n) - \zeta(t_{l-1})]^{1-\alpha} - 11[\zeta(t_n) - \zeta(t_l)]^{1-\alpha}}{[\zeta(t_l) - \zeta(t_{l-1})]} \right] \right. \\ & + \frac{1}{(2-\alpha)} \left[ \frac{[\zeta(t_n) - \zeta(t_{l-1})]^{2-\alpha} - 2[\zeta(t_n) - \zeta(t_l)]^{2-\alpha}}{[\zeta(t_l) - \zeta(t_{l-1})]^2} \right] \\ & \left. + \frac{1}{(2-\alpha)(3-\alpha)} \left[ \frac{[\zeta(t_n) - \zeta(t_{l-1})]^{3-\alpha} - [\zeta(t_n) - \zeta(t_l)]^{3-\alpha}}{[\zeta(t_l) - \zeta(t_{l-1})]^3} \right] \right\}, \end{aligned} \tag{12}$$

$$\begin{aligned} A_{2,n-l} = \alpha_0^{(n)} & \left\{ \frac{1}{2} \left[ \frac{6[\zeta(t_n) - \zeta(t_l)]^{1-\alpha} + [\zeta(t_n) - \zeta(t_{l-1})]^{1-\alpha}}{[\zeta(t_l) - \zeta(t_{l-1})]} \right] \right. \\ & + \frac{1}{(2-\alpha)} \left[ \frac{5[\zeta(t_n) - \zeta(t_l)]^{2-\alpha} - 2[\zeta(t_n) - \zeta(t_{l-1})]^{2-\alpha}}{[\zeta(t_l) - \zeta(t_{l-1})]^2} \right] \\ & \left. + \frac{3}{(2-\alpha)(3-\alpha)} \left[ \frac{[\zeta(t_n) - \zeta(t_l)]^{3-\alpha} - [\zeta(t_n) - \zeta(t_{l-1})]^{3-\alpha}}{[\zeta(t_l) - \zeta(t_{l-1})]^3} \right] \right\}, \end{aligned} \tag{13}$$

$$\begin{aligned} A_{3,n-l} = \alpha_0^{(n)} & \left\{ -\frac{1}{2} \left[ \frac{2[\zeta(t_n) - \zeta(t_{l-1})]^{1-\alpha} + 3[\zeta(t_n) - \zeta(t_l)]^{1-\alpha}}{[\zeta(t_l) - \zeta(t_{l-1})]} \right] \right. \\ & + \frac{1}{(2-\alpha)} \left[ \frac{[\zeta(t_n) - \zeta(t_{l-1})]^{2-\alpha} - 4[\zeta(t_n) - \zeta(t_l)]^{2-\alpha}}{[\zeta(t_l) - \zeta(t_{l-1})]^2} \right] \\ & \left. + \frac{3}{(2-\alpha)(3-\alpha)} \left[ \frac{[\zeta(t_n) - \zeta(t_{l-1})]^{3-\alpha} - [\zeta(t_n) - \zeta(t_l)]^{3-\alpha}}{[\zeta(t_l) - \zeta(t_{l-1})]^3} \right] \right\}, \end{aligned} \tag{14}$$

$$\begin{aligned} A_{4,n-l} = \alpha_0^{(n)} & \left\{ \frac{1}{6} \left[ \frac{[\zeta(t_n) - \zeta(t_{l-1})]^{1-\alpha} + 2[\zeta(t_n) - \zeta(t_l)]^{1-\alpha}}{[\zeta(t_l) - \zeta(t_{l-1})]} \right] \right. \\ & + \frac{1}{(2-\alpha)} \left[ \frac{[\zeta(t_n) - \zeta(t_l)]^{2-\alpha}}{[\zeta(t_l) - \zeta(t_{l-1})]^2} \right] \\ & \left. + \frac{1}{(2-\alpha)(3-\alpha)} \left[ \frac{[\zeta(t_n) - \zeta(t_l)]^{3-\alpha} - [\zeta(t_n) - \zeta(t_{l-1})]^{3-\alpha}}{[\zeta(t_l) - \zeta(t_{l-1})]^3} \right] \right\}, \end{aligned} \tag{15}$$

where  $3 \leq l \leq n$ . After simplifying Equation (11), we obtain the following form

$$\begin{aligned} & \frac{[\omega_n]^{-1}}{\Gamma(1-\alpha)} \sum_{l=3}^n \int_{t_{l-1}}^{t_l} [\zeta(t_n) - \zeta(s)]^{-\alpha} g'(s) ds \\ &= \sum_{l=3}^n [a_{n-l}(g_l - g_{l-1}) + b_{n-l}(g_l - 2g_{l-1} + g_{l-2}) \\ &+ c_{n-l}(g_l - 3g_{l-1} + 3g_{l-2} - g_{l-3})] + E_\tau^n \\ &= \sum_{l=3}^n [a_{n-l}(\nabla_\tau g_l) + b_{n-l}(\nabla_\tau^2 g_l) + c_{n-l}(\nabla_\tau^3 g_l)] + E_\tau^n. \end{aligned} \tag{16}$$

Here, we introduce another coefficient  $c_{n-l}$ , which is defined as

$$\begin{aligned} c_{n-l} = \alpha_0^{(n)} \left\{ \frac{1}{(2-\alpha)(3-\alpha)} \left[ \frac{[\zeta(t_n) - \zeta(t_{l-1})]^{3-\alpha} - [\zeta(t_n) - \zeta(t_l)]^{3-\alpha}}{[\zeta(t_l) - \zeta(t_{l-1})]^3} \right. \right. \\ \left. \left. - \frac{1}{(2-\alpha)} \left[ \frac{[\zeta(t_n) - \zeta(t_l)]^{2-\alpha}}{[\zeta(t_l) - \zeta(t_{l-1})]^2} \right] \right. \right. \\ \left. \left. - \frac{1}{6} \left[ \frac{[\zeta(t_n) - \zeta(t_{l-1})]^{1-\alpha} + 2[\zeta(t_n) - \zeta(t_l)]^{1-\alpha}}{[\zeta(t_l) - \zeta(t_{l-1})]} \right] \right\}, \quad 3 \leq l \leq n, \end{aligned} \tag{17}$$

and coefficients  $a_{n-l}, b_{n-l}$  are defined in Equations (7) and (10), respectively, and Equation (16) gives a more compact form of Equation (11). Such forms of coefficients were missing in [21]. From this we can easily discuss properties of coefficients.

Motivated by [21] (developed for Caputo derivative), a new numerical scheme for the generalized Caputo-type fractional derivative of order  $\alpha$  of the function  $\mathcal{V}(t)$  at grid point  $t_n$ , with the help of Equations (6), (9) and (11), is defined by

$$\begin{aligned} {}^{\mathcal{H}}\mathcal{D}_{t;[\zeta(t),\omega(t)]}^\alpha \mathcal{V}(t)|_{t=t_n} &= \frac{[\omega_n]^{-1}}{\Gamma(1-\alpha)} \int_0^{t_n} \frac{g'(s)}{[\zeta(t_n) - \zeta(s)]^\alpha} ds \\ &= \frac{[\omega_n]^{-1}}{\Gamma(1-\alpha)} \left[ \int_0^{t_1} \frac{g'(s)}{[\zeta(t_n) - \zeta(s)]^\alpha} ds + \int_{t_1}^{t_2} \frac{g'(s)}{[\zeta(t_n) - \zeta(s)]^\alpha} ds \right. \\ &\quad \left. + \sum_{l=3}^n \int_{t_{l-1}}^{t_l} \frac{g'(s)}{[\zeta(t_n) - \zeta(s)]^\alpha} ds \right] \\ &= \sum_{l=0}^n \lambda_l \omega_{n-l} \mathcal{V}_{n-l}, \end{aligned} \tag{18}$$

with  $g(s) = \omega(s)\mathcal{V}(s)$ .

**Lemma 1.** For any  $\alpha \in (0, 1)$  and  $\mathcal{V}(t) \in C^4[0, T]$ , then

$${}^{\mathcal{C}}\mathcal{D}_{t;[\zeta(t),\omega(t)]}^\alpha \mathcal{V}_n = {}^{\mathcal{H}}\mathcal{D}_{t;[\zeta(t),\omega(t)]}^\alpha \mathcal{V}_n + E_\tau^n, \quad n = 1, 2, \dots, N,$$

where,  ${}^{\mathcal{H}}\mathcal{D}_{t;[\zeta(t),\omega(t)]}^\alpha$  is the approximation of GCFD and  $|E_\tau^n| = \mathcal{O}(\tau^{4-\alpha})$ .

For distinct values of  $n$ , the coefficients in (18) can be expressed as below. For  $n = 1$ ,

$$\begin{cases} \lambda_0 = a_0, \\ \lambda_1 = -a_0. \end{cases}$$

For  $n = 2$ ,

$$\begin{cases} \lambda_0 = a_0 + b_0, \\ \lambda_1 = a_1 - a_0 - 2b_0, \\ \lambda_2 = -a_1 + b_0. \end{cases}$$

For  $n = 3$ ,

$$\begin{cases} \lambda_0 = A_{1,0}, \\ \lambda_1 = A_{2,0} + a_1 + b_1, \\ \lambda_2 = A_{3,0} + a_2 - a_1 - 2b_1, \\ \lambda_3 = A_{4,0} - a_2 + b_1. \end{cases}$$

For  $n = 4$ ,

$$\begin{cases} \lambda_0 = A_{1,0}, \\ \lambda_1 = A_{1,1} + A_{2,0}, \\ \lambda_2 = A_{2,1} + A_{3,0} + a_2 + b_2, \\ \lambda_3 = A_{3,1} + A_{4,0} + a_3 - a_2 - 2b_2, \\ \lambda_4 = A_{4,1} - a_3 + b_2. \end{cases}$$

For  $n = 5$ ,

$$\begin{cases} \lambda_0 = A_{1,0}, \\ \lambda_1 = A_{1,1} + A_{2,0}, \\ \lambda_2 = A_{1,2} + A_{2,1} + A_{3,0}, \\ \lambda_3 = A_{2,2} + A_{3,1} + A_{4,0} + a_3 + b_3, \\ \lambda_4 = A_{3,2} + A_{4,1} + a_4 - a_3 - 2b_3, \\ \lambda_5 = A_{4,2} - a_4 + b_3. \end{cases}$$

For  $n \geq 6$ ,

$$\begin{cases} \lambda_0 = A_{1,0}, \\ \lambda_1 = A_{1,1} + A_{2,0}, \\ \lambda_2 = A_{1,2} + A_{2,1} + A_{3,0}, \\ \lambda_l = A_{1,l} + A_{2,l-1} + A_{3,l-2} + A_{4,l-3} \quad (3 \leq l \leq n-3), \\ \lambda_{n-2} = a_{n-2} + b_{n-2} + A_{2,n-3} + A_{3,n-4} + A_{4,n-5}, \\ \lambda_{n-1} = a_{n-1} - a_{n-2} - 2b_{n-2} + A_{3,n-3} + A_{4,n-4}, \\ \lambda_n = -a_{n-1} + b_{n-2} + A_{4,n-3}. \end{cases} \tag{19}$$

**Lemma 2.** *If the scale function  $\zeta$  fulfills (8), and the weight function  $\omega$  is non-negative and non-decreasing on uniform time grids, then*

(i) *Ref. [35] The linear approximation coefficient satisfies,  $1 \leq l \leq n$ ,*

$$0 < a_{n-1} < \dots < a_{n-l} < a_{n-l-1} < \dots < a_1 < a_0.$$

(ii) *The quadratic approximation coefficient satisfies,  $2 \leq l \leq n$ ,*

$$0 < b_{n-2} < \dots < b_{n-l} < b_{n-l-1} < \dots < b_1 < b_0.$$

**Proof.** (i) If scale function  $\zeta$  is continuous on its respective domain then, by using mean-value theorem, there exist  $\hat{x}_l \in (t_{l-1}, t_l)$  such that

$$\frac{1}{\tau} \int_{t_{l-1}}^{t_l} [\zeta(t_n) - \zeta(s)]^{-\alpha} ds = [\zeta(t_n) - \zeta(\hat{x}_l)]^{-\alpha}, \quad 1 \leq l \leq n. \tag{20}$$

Since  $[\zeta(t_n) - \zeta(s)]^{-\alpha}$  is a monotone increasing function, we easily get our required result.

(ii) Let  $\eta(s) = [\zeta(t_n) - \zeta(s)]^{1-\alpha}$ ; suppose scale function  $\zeta$  is sufficiently smooth on domain  $[0, T]$  then mean-value theorem yields

$$\begin{aligned}
 2 \int_{t_{l-1}}^{t_l} \eta(s) ds - (\eta(t_{l-1}) + \eta(t_l)) &= 2\eta(\tilde{x}_l) - (\eta(t_{l-1}) + \eta(t_l)), \quad \tilde{x}_l \in (t_{l-1}, t_l), \\
 &= -\theta(\eta'(t_l) - \eta'(t_{l-1})), \quad 0 < \theta < 1 \\
 &= -\theta\tau\eta''(v_l), \quad v_l \in (t_{l-1}, t_l), \\
 &= \frac{\theta\alpha(1-\alpha)}{\tau} [\zeta(t_l) - \zeta(t_{l-1})]^2 [\zeta(t_n) - \zeta(v_l)]^{-\alpha-1} > 0. \tag{21}
 \end{aligned}$$

Using (21), we can easily get that  $b_{n-l} > 0$  for positive strictly increasing weight function  $\omega(t)$ . Since  $[\zeta(t_n) - \zeta(s)]^{-\alpha-1}$  is a monotone increasing function on temporal domain  $[0, T]$ , so we get the desired result.  $\square$

**Lemma 3.** Suppose that the scale function  $\zeta$  is positive and strictly increasing, and the weight function  $\omega$  is non-negative and non-decreasing, then, for each  $\alpha \in (0, 1)$ , the following conditions hold for coefficients in (19)

- (1)  $\lambda_0 > 0, \forall n \geq 1,$
- (2)  $\sum_{l=0}^n \lambda_l = 0.$

**Proof.** (1) If  $n = 1$ , then

$$\lambda_0 = a_0 = \alpha_0^{(n)} [\zeta_1 - \zeta_0]^{-\alpha},$$

as the scale function is strictly increasing, therefore  $\zeta_{n-1} < \zeta_n$ , for  $n \geq 1$ . This implies that  $\lambda_0 = a_0 > 0$ .

If  $n = 2$ , then  $\lambda_0 = a_0 + b_0$ , since

$$b_0 = \alpha_0^{(n)} \left\{ \left( \frac{1}{2-\alpha} - \frac{1}{2} \right) [\zeta_2 - \zeta_1]^{-\alpha} \right\} > 0,$$

and we have already shown that  $a_0 > 0$ , therefore  $\lambda_0 = a_0 + b_0 > 0$ .

If  $n \geq 3$  then, for  $0 < \alpha < 1$ ,

$$\lambda_0 = A_{1,0} = \alpha_0^{(n)} \left\{ \left( \frac{1}{3} + \frac{1}{(2-\alpha)} + \frac{1}{(2-\alpha)(3-\alpha)} \right) [\zeta_n - \zeta_{n-1}]^{-\alpha} \right\} > 0.$$

(2) If  $n = 1$ , then  $\lambda_0 = -\lambda_1 = a_0 > 0$ , for  $0 < \alpha < 1$ . This implies that  $\lambda_0 + \lambda_1 = 0$ .

If  $n = 2$ , then there exists an  $\alpha \in (0, 1)$ , by numerical analysis

$$\lambda_0 + \lambda_1 + \lambda_2 = (a_0 + b_0) + (a_1 - a_0 + 2b_0) + (-a_1 + b_0) = 0.$$

If  $n \geq 3$ , then

$$\begin{aligned} \sum_{l=0}^n \lambda_l &= A_{1,0} + A_{1,1} + A_{2,0} + A_{1,2} + A_{2,1} + A_{3,0} \\ &+ \sum_{l=3}^{n-3} (A_{1,l} + A_{2,l-1} + A_{3,l-2} + A_{4,l-3}) + a_{n-2} + b_{n-2} \\ &+ A_{2,n-3} + A_{3,n-4} + A_{4,n-5} + a_{n-1} - a_{n-2} - 2b_{n-2} + A_{3,n-3} \\ &+ A_{4,n-4} - a_{n-1} + b_{n-2} + A_{4,n-3} \\ &= \sum_{j=0}^{n-3} (A_{1,j} + A_{2,j} + A_{3,j} + A_{4,j}) = 0. \end{aligned}$$

□

**Lemma 4.** If scale function  $\zeta$  is a Lipschitz function on interval  $[t_{l-1}, t_l]$  with Lipschitz constant  $L$ , then

$$|\zeta_l - \zeta_{l-1}| \leq L\tau, \quad 1 \leq l \leq n.$$

*Truncation Error for Generalized Caputo Derivative Term*

For truncation error of approximation of the generalized Caputo derivative defined in (18), for simplicity, suppose that function  $g(t) = \omega(t)\mathcal{V}(t)$  such that  $g(t) \in C^4((0, T])$  and  $\zeta(t) = v$ ; this implies  $t = \zeta^{-1}(v)$ . Therefore,  $g(v) = \omega(\zeta^{-1}(v))\mathcal{V}(\zeta^{-1}(v))$ .

**Theorem 1.** A triangle inequality gives the bound

$$|\mathcal{D}_{t;[\zeta(t),\omega(t)]}^{\alpha} g_n - {}^{\mathcal{H}}\mathcal{D}_{t;[\zeta(t),\omega(t)]}^{\alpha} g_n| \leq \sum_{n=1}^N |E_{\tau}^n|,$$

with

$$E_{\tau}^n = \frac{[\omega_n]^{-1}}{\Gamma(1-\alpha)} \int_{\zeta_{l-1}}^{\zeta_l} [\zeta_n - v]^{-\alpha} [g(v) - \Pi_l g(v)]' dv, \quad 1 \leq l \leq n.$$

$$(1) |E_{\tau}^1| \leq \frac{\alpha[\omega_n]^{-1}}{\Gamma(1-\alpha)} \left[ \frac{1}{8\alpha} + \frac{1}{2(1-\alpha)(2-\alpha)} \right] \max_{t_0 \leq v_s \leq t_1} |g^{(2)}(v)| L^{2-\alpha} (\tau)^{2-\alpha}, \quad n = 1,$$

$$(2) |E_{\tau}^2| \leq \frac{\alpha[\omega_n]^{-1}}{\Gamma(1-\alpha)} \left\{ \frac{1}{12} \max_{t_0 \leq v_s \leq t_1} |g^{(2)}(v)| (t_2 - t_1)^{-\alpha-1} L^{2-\alpha} (\tau)^3 + \left[ \frac{1}{12} + \frac{1}{3(1-\alpha)(2-\alpha)} \left( \frac{1}{2} + \frac{1}{(3-\alpha)} \right) \right] \max_{t_0 \leq v_s \leq t_2} |g^{(3)}(v)| L^{3-\alpha} (\tau)^{3-\alpha} \right\}, \quad n = 2,$$

$$(3) |E_{\tau}^n| \leq \frac{\alpha[\omega_n]^{-1}}{\Gamma(1-\alpha)} \left\{ \frac{1}{72} \max_{t_0 \leq x \leq t_2} |g^{(3)}(x)| (t_n - t_2)^{-\alpha-1} L^{3-\alpha} (\tau)^4 + \left[ \frac{3}{128\alpha} + \frac{1}{12(1-\alpha)(2-\alpha)} \left( 1 + \frac{3}{(3-\alpha)} + \frac{3}{(3-\alpha)(4-\alpha)} \right) \right] \max_{t_0 \leq x_1 \leq t_n} |g^{(4)}(x_1)| L^{4-\alpha} (\tau)^{4-\alpha} \right\}, \quad n \geq 3.$$

**Proof.** (1) Ref. [23] For  $n = 1$ , the scheme (18) is a linear approximation of the GCFD and the convergence order for this approximation formula is  $\mathcal{O}(\tau^{2-\alpha})$ .

(2) Ref. [23] For  $n = 2$ , the scheme (18) is a quadratic approximation of GCFD and here the convergence order of the approximation formula is  $\mathcal{O}(\tau^{3-\alpha})$ .

(3) For  $n \geq 3$ , by the Lagrange interpolation remainder theorem, we use quadratic interpolation function  $\Pi_2g(v)$  to interpolate  $g(v)$  using node points  $(\zeta_0, g_0), (\zeta_1, g_1), (\zeta_2, g_2)$  on interval  $[\zeta_0, \zeta_2]$  and cubic interpolation function  $\Pi_lg(v)$  depends on  $(\zeta_{l-3}, g_{l-3}), (\zeta_{l-2}, g_{l-2}), (\zeta_{l-1}, g_{l-1}), (\zeta_l, g_l)$  to interpolate  $g(v)$  on  $[\zeta_{l-3}, \zeta_l]$  as follows

$$g(v) - \Pi_2g(v) = \frac{g^{(3)}(\eta_1)}{3!} (v - \zeta_0)(v - \zeta_1)(v - \zeta_2), \text{ vs. } \in [\zeta_0, \zeta_2], \eta_1 \in (\zeta_0, \zeta_2), \tag{22}$$

$$g(v) - \Pi_lg(v) = \frac{g^{(4)}(\eta_l)}{4!} (v - \zeta_{l-3})(v - \zeta_{l-2})(v - \zeta_{l-1})(v - \zeta_l), \text{ vs. } \in [\zeta_{l-3}, \zeta_l], \eta_l \in (\zeta_{l-3}, \zeta_l), \tag{23}$$

where  $3 \leq l \leq n$ .

Now,

$$\begin{aligned} E_\tau^n &= \frac{[\omega_n]^{-1}}{\Gamma(1-\alpha)} \left[ \int_{\zeta_0}^{\zeta_2} [g(v) - \Pi_2g(v)]' [\zeta_n - v]^{-\alpha} dv \right. \\ &\quad \left. + \sum_{l=3}^n \int_{\zeta_{l-1}}^{\zeta_l} [g(v) - \Pi_lg(v)]' [\zeta_n - v]^{-\alpha} dv \right] \\ &= \frac{[\omega_n]^{-1}}{\Gamma(1-\alpha)} \left\{ [g(v) - \Pi_2g(v)] [\zeta_n - v]^{-\alpha} \Big|_{\zeta_0}^{\zeta_2} \right. \\ &\quad - \alpha \int_{\zeta_0}^{\zeta_2} [g(v) - \Pi_2g(v)] [\zeta_n - v]^{-\alpha-1} dv \\ &\quad + \sum_{l=3}^n \left[ [g(v) - \Pi_lg(v)] [\zeta_n - v]^{-\alpha} \Big|_{\zeta_{l-1}}^{\zeta_l} \right. \\ &\quad \left. - \alpha \int_{\zeta_{l-1}}^{\zeta_l} [g(v) - \Pi_lg(v)] [\zeta_n - v]^{-\alpha-1} dv \right] \left. \right\} \\ &= -\frac{\alpha [\omega_n]^{-1}}{\Gamma(1-\alpha)} \left\{ \int_{\zeta_0}^{\zeta_2} [g(v) - \Pi_2g(v)] [\zeta_n - v]^{-\alpha-1} dv \right. \\ &\quad \left. + \sum_{l=3}^n \int_{\zeta_{l-1}}^{\zeta_l} [g(v) - \Pi_lg(v)] [\zeta_n - v]^{-\alpha-1} dv \right\} \tag{24} \end{aligned}$$

Since, from (22) and (23),

$$\begin{aligned} [g(v) - \Pi_2g(v)] [\zeta_n - v]^{-\alpha} \Big|_{\zeta_0}^{\zeta_2} &= \frac{g^{(3)}(\eta_1)}{3!} (v - \zeta_0)(v - \zeta_1)(v - \zeta_2) [\zeta_n - v]^{-\alpha} \Big|_{\zeta_0}^{\zeta_2} = 0, \\ [g(v) - \Pi_lg(v)] [\zeta_n - v]^{-\alpha} \Big|_{\zeta_{l-1}}^{\zeta_l} &= \frac{g^{(4)}(\eta_l)}{4!} (v - \zeta_{l-3})(v - \zeta_{l-2})(v - \zeta_{l-1})(v - \zeta_l) \Big|_{\zeta_{l-1}}^{\zeta_l} = 0. \end{aligned}$$

Consider the first integration of Equation (24)

$$\begin{aligned} &\left| \int_{\zeta_0}^{\zeta_2} [g(v) - \Pi_2(v)] [\zeta_n - v]^{-\alpha-1} dv \right| \\ &= \left| \int_{\zeta_0}^{\zeta_2} \frac{g^{(3)}(\eta_1)}{3!} (v - \zeta_0)(v - \zeta_1)(v - \zeta_2) [\zeta_n - v]^{-\alpha-1} dv \right| \\ &\leq \frac{1}{6} \max_{\zeta_0 \leq \eta_1 \leq \zeta_2} |g^{(3)}(\eta_1)| (\zeta_n - \zeta_2)^{-\alpha-1} \frac{(\zeta_0 - \zeta_2)^3 (\zeta_0 - 2\zeta_1 + \zeta_2)}{12} \\ &\leq \frac{1}{6} \max_{\zeta_0 \leq \eta_1 \leq \zeta_2} |g^{(3)}(\eta_1)| (\zeta_n - \zeta_2)^{-\alpha-1} \frac{(\zeta_0 - \zeta_2)^3 (\zeta_0 - \zeta_1)}{12}. \end{aligned}$$

Using Lemma (4), we have the following inequality

$$\left| \int_{\zeta_0}^{\zeta_2} [g(v) - \Pi_2g(v)] [\zeta_n - v]^{-\alpha-1} dv \right| \leq \frac{1}{72} \max_{t_0 \leq x \leq t_2} |g^{(3)}(x)| (t_n - t_2)^{-\alpha-1} L^{3-\alpha}(\tau)^4. \tag{25}$$

Consider the second integration of Equation (24)

$$\begin{aligned} & \left| \sum_{l=3}^n \int_{\zeta_{l-1}}^{\zeta_l} [g(v) - \Pi_l g(v)] [\zeta_n - v]^{-\alpha-1} dv \right| \\ & \leq \left| \sum_{l=3}^{n-1} \int_{\zeta_{l-1}}^{\zeta_l} \frac{g^{(4)}(\eta_l)}{4!} (v - \zeta_{l-3})(v - \zeta_{l-2})(v - \zeta_{l-1})(v - \zeta_l) [\zeta_n - v]^{-\alpha-1} dv \right| \\ & \quad + \left| \int_{\zeta_{n-1}}^{\zeta_n} \frac{g^{(4)}(\eta_n)}{4!} (v - \zeta_{n-3})(v - \zeta_{n-2})(v - \zeta_{n-1})(v - \zeta_n) [\zeta_n - v]^{-\alpha-1} dv \right|. \end{aligned} \tag{26}$$

Consider the first part of the RHS of Equation (26)

$$\begin{aligned} & \left| \sum_{l=3}^{n-1} \int_{\zeta_{l-1}}^{\zeta_l} \frac{g^{(4)}(\eta_l)}{4!} (v - \zeta_{l-3})(v - \zeta_{l-2})(v - \zeta_{l-1})(v - \zeta_l) [\zeta_n - v]^{-\alpha-1} dv \right| \\ & \leq \frac{1}{24} \max_{\zeta_2 \leq \eta_2 \leq \zeta_{n-1}} |g^{(4)}(\eta_2)| \tilde{f}(\zeta_{l-3}, \zeta_{l-2}, \zeta_{l-1}, \zeta_l) \int_{\zeta_2}^{\zeta_{n-1}} [\zeta_n - v]^{-\alpha-1} dv \\ & \leq \frac{1}{24\alpha} \max_{\zeta_2 \leq \eta_2 \leq \zeta_{n-1}} |g^{(4)}(\eta_2)| \tilde{f}(\zeta_{l-3}, \zeta_{l-2}, \zeta_{l-1}, \zeta_l) (\zeta_n - \zeta_{n-1})^{-\alpha}. \end{aligned}$$

Here,  $\tilde{f}(\zeta_{l-3}, \zeta_{l-2}, \zeta_{l-1}, \zeta_l)$  is the  $\max_{\zeta_2 \leq v_s \leq \zeta_{n-1}} [(v - \zeta_{l-3})(v - \zeta_{l-2})(v - \zeta_{l-1})(v - \zeta_l)]$ . Using Lemma 4, we get the following inequality

$$\begin{aligned} & \left| \sum_{l=3}^{n-1} \int_{\zeta_{l-1}}^{\zeta_l} \frac{g^{(4)}(\eta_l)}{4!} (v - \zeta_{l-3})(v - \zeta_{l-2})(v - \zeta_{l-1})(v - \zeta_l) [\zeta_n - v]^{-\alpha-1} dv \right| \\ & \leq \frac{3}{128\alpha} \max_{t_2 \leq x_1 \leq t_{n-1}} |g^{(4)}(x_1)| L^{4-\alpha} (\tau)^{4-\alpha}. \end{aligned} \tag{27}$$

**Remark 3.** If scale function  $\zeta$  fulfills the condition of the Lipschitz function such that  $|\zeta_l - \zeta_{l-1}| \leq L\tau$ , then  $\max_{\zeta_2 \leq v_s \leq \zeta_{n-1}} |(v - \zeta_{l-3})(v - \zeta_{l-2})(v - \zeta_{l-1})(v - \zeta_l)|$  is obtained at  $v = \zeta_{l-2} + \frac{L\tau}{2}$ , therefore

$$\tilde{f}(\zeta_{l-3}, \zeta_{l-2}, \zeta_{l-1}, \zeta_l) = \max_{\zeta_2 \leq v_s \leq \zeta_{n-1}} [(v - \zeta_{l-3})(v - \zeta_{l-2})(v - \zeta_{l-1})(v - \zeta_l)] \leq \frac{9}{16} L^4 (\tau)^4.$$

Consider the second part of the RHS of Equation (26)

$$\begin{aligned} & \left| \int_{\zeta_{n-1}}^{\zeta_n} \frac{g^{(4)}(\eta_n)}{4!} (v - \zeta_{n-3})(v - \zeta_{n-2})(v - \zeta_{n-1})(v - \zeta_n) [\zeta_n - v]^{-\alpha-1} dv \right| \\ & \leq \frac{1}{24} \max_{\zeta_{n-1} \leq \eta_3 \leq \zeta_n} |g^{(4)}(\eta_3)| \left| \int_{\zeta_{n-1}}^{\zeta_n} (v - \zeta_{n-3})(v - \zeta_{n-2})(v - \zeta_{n-1}) [\zeta_n - v]^{-\alpha} dv \right| \\ & \leq \frac{1}{12(1-\alpha)(2-\alpha)} \left( 1 + \frac{3}{(3-\alpha)} + \frac{3}{(3-\alpha)(4-\alpha)} \right) \max_{\zeta_{n-1} \leq \eta_3 \leq \zeta_n} |g^{(4)}(\eta_3)| (\zeta_n - \zeta_{n-1})^{4-\alpha} \\ & \leq \frac{1}{12(1-\alpha)(2-\alpha)} \left( 1 + \frac{3}{(3-\alpha)} + \frac{3}{(3-\alpha)(4-\alpha)} \right) \max_{t_{n-1} \leq x_2 \leq t_n} |g^{(4)}(x_2)| L^{4-\alpha} (\tau)^{4-\alpha}. \end{aligned} \tag{28}$$

Now combining (25), (27) and (28), then the error bound is

$$\begin{aligned} |E_\tau^n| & \leq \frac{\alpha [\omega_n]^{-1}}{\Gamma(1-\alpha)} \left\{ \frac{1}{72} \max_{t_0 \leq x \leq t_2} |g^{(3)}(x)| (t_n - t_2)^{-\alpha-1} L^{3-\alpha} (\tau)^4 \right. \\ & \quad + \left[ \frac{3}{128\alpha} + \frac{1}{12(1-\alpha)(2-\alpha)} \left( 1 + \frac{3}{(3-\alpha)} \right. \right. \\ & \quad \left. \left. + \frac{3}{(3-\alpha)(4-\alpha)} \right) \right] \max_{t_0 \leq x_1 \leq t_n} |g^{(4)}(x_1)| L^{4-\alpha} (\tau)^{4-\alpha} \left. \right\}. \end{aligned} \tag{29}$$

□

### 3. Numerical Scheme for the Generalized Fractional Advection–Diffusion Equation

In this section, we study the numerical scheme for solving the generalized fractional advection–diffusion equation defined by (1).

Let  $u(x, t) = \omega(t)U(x, t) - \omega(0)U_0(x)$ . We rewrite Equation (1) to a similar equation using a unity weight function and the same scale function  $\zeta(t)$ . Then, Equation (1) converts into the following form:

$$\begin{cases} {}_0^C \mathcal{D}_{t;[\zeta(t),1]}^\alpha u(x, t) = D \frac{\partial^2 u(x,t)}{\partial x^2} - A \frac{\partial u(x,t)}{\partial x} + f(x, t), & x \in \Omega, \quad t \in (0, T], \\ u(x, 0) = 0, & x \in \bar{\Omega} = \Omega \cup \partial\Omega, \\ u(0, t) = \phi_1(t), \quad u(a, t) = \phi_2(t), & t \in (0, T], \end{cases} \tag{30}$$

where  $\phi_1(t) = \omega(t)\rho_1(t) - \omega(0)\rho_1(0)$ ,  $\phi_2(t) = \omega(t)\rho_2(t) - \omega(0)\rho_2(0)$ , and  $f(x, t) = D\omega(0)U_0''(x) - A\omega(0)U_0'(x) + \omega(t)g(x, t)$ .

For the uniform spatial mesh, let  $0 = x_0 < x_1 < \dots < x_M = a$  of the interval  $[0, a]$  with step size  $h = \frac{a}{M}$  where  $M$  denotes number of subintervals, the grid points  $x_0 + ih$  ( $0 \leq i \leq M$ ), and  $\tau = \frac{T}{N}$  be the step size in the temporal direction with grids  $t_n = n\tau$  ( $0 = t_0 < t_1 < \dots < t_n = T$ ).

Now, we discretize our problem (30) at  $(x_i, t_n)$ , then we get

$${}_0^C \mathcal{D}_{t;[\zeta(t),1]}^\alpha u(x_i, t_n) = Du_{xx}(x_i, t_n) - Au_x(x_i, t_n) + f(x_i, t_n). \tag{31}$$

In Equation (31), for fixed  $t_n$  and  $1 \leq i \leq M - 1$ , the first- and second-order spatial derivatives are discretized by using the following central difference approximations:

$$\frac{\partial u(x_i, t_n)}{\partial x} = \frac{u_n^{i+1} - u_n^{i-1}}{2h} + \mathcal{O}(h^2), \tag{32}$$

$$\frac{\partial^2 u(x_i, t_n)}{\partial x^2} = \frac{u_n^{i+1} - 2u_n^i + u_n^{i-1}}{h^2} + \mathcal{O}(h^2). \tag{33}$$

With the help of Equation (18), we get an approximation of the generalized Caputo-type fractional derivative term in (31) as follows:

$$\begin{aligned} {}^H \mathcal{D}_{t;[\zeta(t),1]}^\alpha u(x_i, t_n) &= \lambda_0 u(x_i, t_n) + \lambda_1 u(x_i, t_{n-1}) + \lambda_2 u(x_i, t_{n-2}) + \sum_{l=3}^{n-3} \lambda_{n-l} u(x_i, t_l) \\ &+ \lambda_{n-2} u(x_i, t_2) + \lambda_{n-1} u(x_i, t_1) + \lambda_n u(x_i, t_0) + \mathcal{O}(\tau^{4-\alpha}). \end{aligned} \tag{34}$$

where  $\lambda_l$  is defined in Equation (19). Next, we use Equations (32)–(34) in discretized Equation (31), yielding

$$\sum_{l=0}^n \lambda_{n-l} u(x_i, t_l) = Du_{xx}(x_i, t_n) - Au_x(x_i, t_n) + f_n^i + e_n^i. \tag{35}$$

where  $|e_n^i| \leq \tilde{c}(\tau^{4-\alpha} + h^2)$  for some constant  $\tilde{c}$ .

Now, we use a numerical approximation  $u_n^i$  of  $u(x_i, t_n)$  to neglect the truncation error term in Equation (35), then we determine the following finite difference scheme:

$$\begin{aligned} \lambda_0 u_n^i + \lambda_1 u_{n-1}^i + \sum_{l=3}^{n-2} \lambda_{n-l} u_l^i + \lambda_{n-2} u_2^i + \lambda_{n-1} u_1^i + \lambda_n u_0^i &= D \frac{u_n^{i+1} - 2u_n^i + u_n^{i-1}}{h^2} \\ &- A \frac{u_n^{i+1} - u_n^{i-1}}{2h} + f_n^i, \end{aligned} \tag{36}$$

where  $1 \leq n \leq N$ ,  $1 \leq i \leq M - 1$ . That is,

$$\begin{cases} (\frac{D}{h^2} + \frac{A}{2h})u_1^{i-1} - (\lambda_0 + \frac{2D}{h^2})u_1^i + (\frac{D}{h^2} - \frac{A}{2h})u_1^{i+1} = \lambda_1 u_0^i - f_1^i, & n = 1, \\ (\frac{D}{h^2} + \frac{A}{2h})u_2^{i-1} - (\lambda_0 + \frac{2D}{h^2})u_2^i + (\frac{D}{h^2} - \frac{A}{2h})u_2^{i+1} = \lambda_1 u_1^i + \lambda_2 u_0^i - f_2^i, & n = 2, \\ (\frac{D}{h^2} + \frac{A}{2h})u_n^{i-1} - (\lambda_0 + \frac{2D}{h^2})u_n^i + (\frac{D}{h^2} - \frac{A}{2h})u_n^{i+1} = \lambda_1 u_{n-1}^i + \sum_{l=0}^{n-2} \lambda_{n-l} u_l^i - f_n^i, & n \geq 3. \end{cases} \tag{37}$$

$$\begin{cases} u_0^i = 0, & 0 \leq i \leq M, \\ u_n^0 = \phi_1(t_n), \quad u_n^M = \phi_2(t_n), & 0 \leq n \leq N. \end{cases}$$

We rewrite the matrix form of the above equation as follows:

$$\begin{cases} KU_1 = \lambda_1 U_0 - F_1 + H_1, & n = 1, \\ KU_2 = \lambda_1 U_1 + \lambda_2 U_0 - F_2 + H_2, & n = 2, \\ KU_n = \lambda_1 U_{n-1} + \sum_{l=0}^{n-2} \lambda_{n-l} U_l - F_n + H_n, & n \geq 3, \end{cases} \tag{38}$$

where the matrix as well as vectors of Equation (38) are defined as follows:

$$K = tri \left[ \frac{D}{h^2} + \frac{A}{2h}, -\lambda_0 - \frac{2D}{h^2}, \frac{D}{h^2} - \frac{A}{2h} \right]_{(M-1) \times (M-1)},$$

$$U_n = (u_n^1, u_n^2, \dots, u_n^{M-1})^T,$$

$$F_n = (f_n^1, f_n^2, \dots, f_n^{M-1})^T,$$

$$H_n = \left( (-\frac{D}{h^2} - \frac{A}{2h})u_n^0, 0, \dots, 0, (-\frac{D}{h^2} + \frac{A}{2h})u_n^M \right)^T, \quad 1 \leq n \leq N.$$

**Remark 4.** Since the coefficient matrix  $A$  is a tridiagonal and strictly diagonally dominant then  $\det(A) \neq 0$  (Levy–Desplanques theorem). Therefore, at each time level  $t_n$ , the proposed scheme (37) has a unique solution for  $1 \leq n \leq N$ .

**Theorem 2.** The local truncation error of difference scheme (36) at  $(x_i, t_n)$ ,  $1 \leq i \leq M - 1$ ,  $1 \leq n \leq N$ , is

$$|e_n^i| \leq C(h^2 + \tau^{4-\alpha}), \tag{39}$$

where  $C$  is the positive constant independent of the time and space step sizes.

**Proof.** From Equations (4.7) the LTE of difference scheme (36) is

$$\begin{aligned} e_n^i &= \lambda_0 u(x_i, t_n) + \lambda_1 u(x_i, t_{n-1}) + \lambda_2 u(x_i, t_{n-2}) + \sum_{l=3}^{n-3} \lambda_{n-l} u(x_i, t_l) + \lambda_{n-2} u(x_i, t_2) \\ &\quad + \lambda_{n-1} u(x_i, t_1) + \lambda_n u(x_i, t_0) - D \frac{u_n^{i+1} - 2u_n^i + u_n^{i-1}}{h^2} + A \frac{u_n^{i+1} - u_n^{i-1}}{2h} - f_n^i \\ &= \left[ \lambda_0 u(x_i, t_n) + \lambda_1 u(x_i, t_{n-1}) + \lambda_2 u(x_i, t_{n-2}) + \sum_{l=2}^{n-3} \lambda_{n-l} u(x_i, t_l) + \lambda_{n-1} u(x_i, t_1) \right. \\ &\quad \left. + \lambda_n u(x_i, t_0) - {}^{\mathcal{H}}\mathcal{D}_{t;[\zeta(t),1]}^\alpha u(x_i, t_n) \right] - D \left[ \frac{u_n^{i+1} - 2u_n^i + u_n^{i-1}}{h^2} - \frac{\partial^2 u(x_i, t_n)}{\partial x^2} \right] \\ &\quad + A \left[ \frac{u_n^{i+1} - u_n^{i-1}}{2h} - \frac{\partial u(x_i, t_n)}{\partial x} \right] \\ &= \mathcal{O}(\tau^{4-\alpha}) - D \mathcal{O}(h^2) + A \mathcal{O}(h^2) = \mathcal{O}(\tau^{4-\alpha} + h^2). \end{aligned}$$

□

In the next theorem, we use  $L^2(\Omega)$ -space with the norm  $\|\cdot\|_2$  and the inner product  $\langle \cdot, \cdot \rangle$ .

**Theorem 3.** (see [22]) *If the tridiagonal matrix elements satisfy the inequality*

$$\lambda_1 \leq (\lambda_0)^{M-3} \left( \lambda_0 + \frac{D}{h^2} - \frac{A}{2h} \right) \left( \lambda_0 + \frac{D}{h^2} + \frac{A}{2h} \right), \tag{40}$$

then the finite difference scheme is stable.

**Proof.** Equation (38) can be rewritten as follows, for  $1 \leq n \leq N$

$$KU_n = \lambda_1 U_{n-1} + \sum_{l=0}^{n-2} \lambda_{n-l} U_l - F_n + H_n,$$

let,  $V_n = \sum_{l=0}^{n-2} \lambda_{n-l} U_l - F_n + H_n$ .

Since matrix  $K$  is invertible then the above equation can be rewritten as

$$U_n = \lambda_1 K^{-1} U_{n-1} + K^{-1} V_n.$$

Using the recurrence relation, we get the following equation

$$\begin{aligned} U_n &= (\lambda_1 K^{-1})^2 U_{n-2} + (\lambda_1 K^{-1}) K^{-1} V_{n-1} + K^{-1} V_n \\ &= (\lambda_1 K^{-1})^n U_0 + (\lambda_1 K^{-1})^{n-1} K^{-1} V_1 + (\lambda_1 K^{-1})^{n-2} K^{-1} V_2 + \dots + K^{-1} V_n. \end{aligned} \tag{41}$$

Let  $\tilde{U}_n$  be the approximate solution of Equation (38), then we define the error at grid point  $t_n = n\tau$

$$e_n = U_n - \tilde{U}_n, \quad 0 \leq n \leq N.$$

Then, we obtain

$$e_n = (\lambda_1 K^{-1})^n e_0, \quad 1 \leq n \leq N.$$

From the definition of the compatible matrix norm

$$\|e_n\| \leq \|(\lambda_1 K^{-1})^n\| \|e_0\|.$$

Since

$$\|(\lambda_1 K^{-1})^n\| \leq \|(\lambda_1 K^{-1})\| \|(\lambda_1 K^{-1})^{n-1}\| \leq \dots \leq \|(\lambda_1 K^{-1})\|^n.$$

According to the Ostrowski theorem ([40], Theorem 3.1), let  $K = [a_{i,j}]_{M-1 \times M-1}$ , then the determinant of  $K$  satisfies

$$\begin{aligned} |\det(K)| &\geq \prod_{i=1}^{M-1} \left( |a_{i,i}| - \sum_{j=1, j \neq i}^{M-1} |a_{i,j}| \right) \\ &= (\lambda_0)^{M-3} \left( \lambda_0 + \frac{D}{h^2} - \frac{A}{2h} \right) \left( \lambda_0 + \frac{D}{h^2} + \frac{A}{2h} \right). \end{aligned} \tag{42}$$

Using assumed inequality (40) into (42), we get  $|\det(K^{-1})| \leq \frac{1}{\lambda_1}$ ; this implies that

$$|\lambda_1| \|K^{-1}\| \leq 1.$$

Therefore,

$$|e_n| \leq |e_0|.$$

Thus, the numerical scheme is stable.  $\square$

**Theorem 4.** The solution  $U_n^i$  of the difference scheme (36) satisfies

$$\max_{i,n} |U(x_i, t_n) - \tilde{U}(x_i, t_n)| \leq C(h^2 + \tau^{4-\alpha}) \tag{43}$$

for some constant  $C$ .

**Proof.** The truncation error for the difference scheme at  $(x_i, t_n) \in [0, a] \times [0, T]$  is

$$|e_n^i| \leq C(h^2 + \tau^{4-\alpha})$$

by Theorem 2. Now, using the theorem of stability, it implies

$$\max_{i,n} |U(x_i, t_n) - \tilde{U}(x_i, t_n)| \leq C|U(x_i, t_0) - \tilde{U}(x_i, t_0)| \tag{44}$$

We obtain the desired result easily after using the truncation error as discussed in Theorem 2.  $\square$

#### 4. Numerical Results

In this section, we will check the numerical accuracy of the proposed schemes (18) and difference scheme (37), and also verify the theoretical convergence order discussed in Theorem 4. Here, we provide three examples to numerically support our theory; in the first example we check the convergence order and absolute error of approximation for the GCFD, while the last two problems get the form (30) to describe the accuracy and maximum absolute error of the difference scheme. All numerical results are implemented in MATLAB R2018b.

To calculate the maximum absolute error  $E_\infty$  and error  $E_2$  corresponding to the  $L_2$ -norm, we use the following formulas [19,21,39], respectively, due to the fact that the exact solutions of the considered test problems are known.

$$E_\infty(M, N) = \max_{1 \leq i \leq M-1} |U_N^i - u_N^i|, \tag{45}$$

$$E_2(M, N) = \left( h \sum_{i=1}^{M-1} |U_N^i - u_N^i|^2 \right)^{1/2}, \tag{46}$$

where  $\{U_n^i\}$  is the exact solution of advection diffusion equation and  $\{u_n^i\}$  is the approximate solution at the point  $(x_i, t_n)$ .

Moreover, the convergence order in the space and time directions for the described difference scheme corresponding to  $L_\infty$ -norm can be evaluated using the following formulas.  $R_x$  is the order of convergence on the space side and  $R_t$  on the temporal side.

$$R_x = \frac{\log(E(2M, N)) - \log(E(M, N))}{\log(2)},$$

and

$$R_t = \frac{\log(E(M, 2N)) - \log(E(M, N))}{\log(2)}.$$

**Example 1.** Ref. [39] Take function  $u(t) = t^{4+\alpha}$ ,  $t \in [0, 1]$ , for  $0 < \alpha < 1$ . Determine the  $\alpha$ -th order GCFD for  $u(t)$  at  $T = 1$  numerically.

The maximum absolute error and rate of convergence for the scheme (18) to approximate the GCFD of function  $u(t)$  for  $\alpha = 0.2, 0.5, 0.8$  with uniform time steps  $1/10, 1/20, 1/40, 1/80, 1/160$  are calculated and shown in the following tables.

Table 1 shows the errors with respect to  $L_\infty$ -norm and convergence rates in time, and these data are found after calculating the classical Caputo derivative (i.e., taking

$\zeta(t) = t, \omega(t) = 1$ ) of function  $u(t)$  with the help of scheme (18). From this table, we can see that the errors of our scheme (18) obtained from the GCFD approximation are lesser compared to the scheme developed in Gao et al. [39] for approximation of the Caputo derivative and the convergence rate of our scheme is  $(4 - \alpha)$ , while accuracy for the time derivative in [39] is  $(3 - \alpha)$ . In Table 2, to compute the maximum errors  $E_\infty$  and order of convergence in the time direction, we take  $\omega(t) = e^t$  while the scale function is fixed with  $t$ . From Table 3, we validate the convergence for  $\zeta(t) = t, \omega(t) = t + 1$  and the CPU time in seconds for  $\alpha = 0.8$  are discussed. Table 4 shows maximum errors and order of convergence for different choices of weight  $\omega(t) = t^{0.5}, t, t^4, e^{2t}$ ; scale is  $\zeta(t) = t$  and  $\alpha = 1/3$ . In all cases, accuracy in time is obtained as  $(4 - \alpha)$  for scheme (18), which is higher than [28,40].

**Table 1.**  $E_\infty$  errors and convergence rates  $R_t$  for Example 1, when  $\zeta(t) = t, \omega(t) = 1$ , with different  $\alpha$ s.

N	$\alpha = 0.2$		$\alpha = 0.5$		$\alpha = 0.5$ [39]	
	$E_\infty$ Error	$R_t$	$E_\infty$ Error	$R_t$	$E_\infty$ Error	$R_t$
10	$1.6978 \times 10^{-4}$		$1.5401 \times 10^{-3}$		$1.3507 \times 10^{-2}$	
20	$1.3130 \times 10^{-5}$	3.6928	$1.4383 \times 10^{-4}$	3.4206	$2.6121 \times 10^{-3}$	2.3704
40	$9.9792 \times 10^{-7}$	3.7178	$1.3116 \times 10^{-5}$	3.4550	$4.8618 \times 10^{-4}$	2.4256
80	$7.4966 \times 10^{-8}$	3.7346	$1.1811 \times 10^{-6}$	3.4731	$8.8645 \times 10^{-5}$	2.4554
160	$5.5944 \times 10^{-9}$	3.7442	$1.0560 \times 10^{-7}$	3.4835	$1.5975 \times 10^{-5}$	2.4722

**Table 2.**  $E_\infty$  errors and convergence rates  $R_t$  for Example 1, when  $\zeta(t) = t, \omega(t) = e^t$ , with different  $\alpha$ s.

N	$\alpha = 0.2$		$\alpha = 0.5$		$\alpha = 0.8$		$\alpha = 0.8$
	$E_\infty$ Error	$R_t$	$E_\infty$ Error	$R_t$	$E_\infty$ Error	$R_t$	CPU Time (s)
10	$7.5552 \times 10^{-4}$		$6.3075 \times 10^{-3}$		$3.2184 \times 10^{-2}$		11.354861
20	$7.1075 \times 10^{-5}$	3.4101	$6.7873 \times 10^{-4}$	3.2162	$4.2148 \times 10^{-3}$	2.9328	33.306962
40	$5.9370 \times 10^{-6}$	3.5815	$6.6677 \times 10^{-5}$	3.3476	$5.0375 \times 10^{-4}$	3.0647	82.772072
80	$4.6934 \times 10^{-7}$	3.6610	$6.2491 \times 10^{-6}$	3.4155	$5.7497 \times 10^{-5}$	3.1312	180.064565
160	$3.5650 \times 10^{-8}$	3.7186	$5.7027 \times 10^{-7}$	3.4539	$6.4090 \times 10^{-6}$	3.1653	419.978865

**Table 3.**  $E_\infty$  errors and convergence rates  $R_t$  for Example 1, when  $\zeta(t) = t, \omega(t) = t + 1$ , with different  $\alpha$ s.

N	$\alpha = 0.2$		$\alpha = 0.5$		$\alpha = 0.8$		$\alpha = 0.8$
	$E_\infty$ Error	$R_t$	$E_\infty$ Error	$R_t$	$E_\infty$ Error	$R_t$	CPU Time (s)
10	$3.5019 \times 10^{-4}$		$3.1752 \times 10^{-3}$		$1.7251 \times 10^{-2}$		10.194270
20	$3.0621 \times 10^{-5}$	3.5155	$3.1426 \times 10^{-4}$	3.3368	$2.0904 \times 10^{-3}$	3.0448	25.931157
40	$2.4466 \times 10^{-6}$	3.6457	$2.9499 \times 10^{-5}$	3.4132	$2.3982 \times 10^{-4}$	3.1238	65.689186
80	$1.8844 \times 10^{-7}$	3.6986	$2.6976 \times 10^{-6}$	3.4509	$2.6799 \times 10^{-5}$	3.1617	155.623905
160	$1.4248 \times 10^{-8}$	3.7252	$2.4326 \times 10^{-7}$	3.4711	$2.9560 \times 10^{-6}$	3.1805	384.953845

**Table 4.**  $E_\infty$  errors and convergence rates  $R_t$  for Example 1, when  $\zeta(t) = t, \alpha = \frac{1}{3}$ , with different weight functions.

N	$\omega(t) = t^{0.5}$		$\omega(t) = t$		$\omega(t) = t^4$		$\omega(t) = e^{2t}$
	$E_\infty$ Error	$R_t$	$E_\infty$ Error	$R_t$	$E_\infty$ Error	$R_t$	$R_t$
10	$9.5450 \times 10^{-4}$		$1.7465 \times 10^{-3}$		$3.2557 \times 10^{-2}$		
20	$8.4374 \times 10^{-5}$	3.4999	$1.5027 \times 10^{-4}$	3.5388	$2.0348 \times 10^{-3}$	4.0000	3.2332
40	$7.0877 \times 10^{-6}$	3.5734	$1.2845 \times 10^{-5}$	3.5483	$1.2749 \times 10^{-4}$	3.9964	3.4225
80	$5.8166 \times 10^{-7}$	3.6071	$1.0650 \times 10^{-6}$	3.5923	$1.1169 \times 10^{-5}$	3.5129	3.5220
160	$4.7123 \times 10^{-8}$	3.6257	$8.6813 \times 10^{-8}$	3.6167	$9.3941 \times 10^{-7}$	3.5716	3.5764

Figure 1a,b show that the comparison of absolute error for the scheme defined in [39] and the current scheme (18) for  $\alpha = 0.5$  and  $\alpha = 0.8$ , respectively.

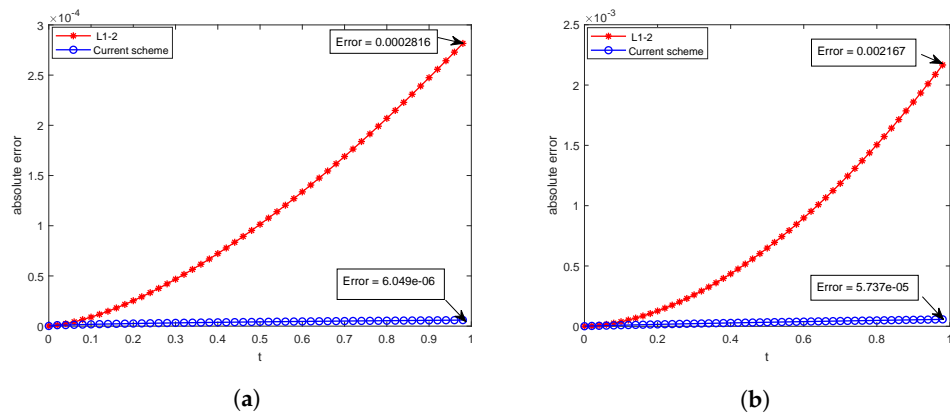


Figure 1. Error plot of the numerical results for Example 1 at final time  $T = 1$  for different values of  $\alpha$  (left side (a) for  $\alpha = 0.5$ ; right side (b) for  $\alpha = 0.8$ ).

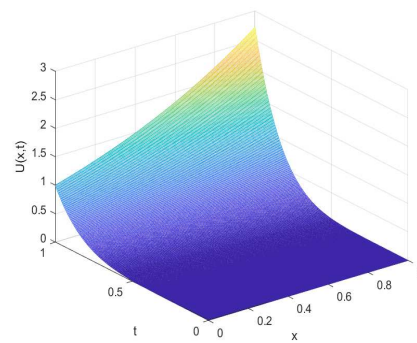
Example 2. Ref. [21] We take the following generalized fractional advection–diffusion equation:

$$\begin{cases} {}_0^C \mathcal{D}_{t;[\zeta(t),\omega(t)]}^\alpha u(x,t) = \frac{\partial^2 u(x,t)}{\partial x^2} - \frac{\partial u(x,t)}{\partial x} + f(x,t), & (x,t) \in (0,1) \times (0,1), \\ u(x,0) = 0, & x \in (0,1), \\ u(0,t) = t^{6+\alpha}, u(1,t) = et^{6+\alpha}, & t \in (0,1], \end{cases}$$

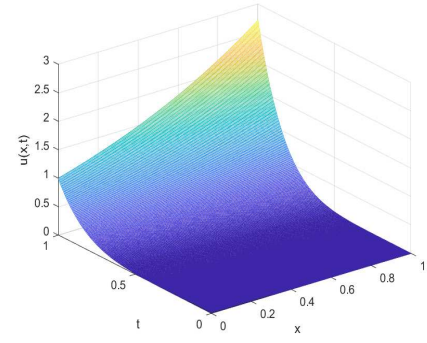
where  $f(x,t) = e^x t^6 \frac{\Gamma(7+\alpha)}{720}$ . When  $\zeta(t) = t$  and  $\omega(t) = 1$ , then  $u(x,t) = e^x t^{6+\alpha}$  is the exact solution.

To solve this example, we use the numerical scheme defined in (37). The maximum errors at time  $t = 1$  for different values of  $\alpha$  with different step sizes, and rate of convergence in time direction and space direction are displayed in Tables 5 and 6. In Table 5, we set  $h = \frac{1}{2000}$  and describe the numerical errors and convergence rates in time  $R_t$  for different values of  $N$ . In Table 6, we fix  $\tau = \frac{1}{500}$  and present the numerical errors and spatial convergence rates  $R_x$  for different values of  $M$ . It is shown that our scheme (37) gives  $(4 - \alpha)$ -order convergence in the temporal direction and second-order convergence in the spatial direction.

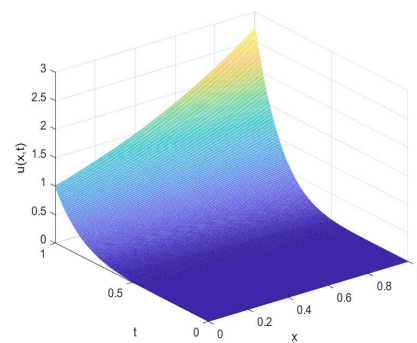
Figure 2 represents the exact and numerical solution of the Example 2 for different values of  $\alpha$ .



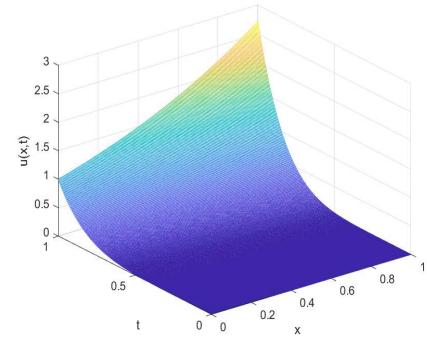
(a) Exact solution for  $\alpha = 0.95$



(b) Numerical solution for  $\alpha = 0.95$



(c) Numerical solution for  $\alpha = 0.6$



(d) Numerical solution for  $\alpha = 0.45$

**Figure 2.** Exact and approximate solutions of Example 2 for different  $\alpha$ 's with  $M = N = 200$ ,  $\omega(t) = 1$ ,  $\zeta(t) = t$ .

**Table 5.** Errors  $E_\infty$  and  $E_2$  with convergence rates in time for Example 2, when  $h = 1/2000$  with different  $\alpha$ s.

$\alpha$	$N$	$E_\infty$ Error	$R_t$	$E_2$ Error	$R_t$
0.8	8	$1.6385 \times 10^{-2}$		$7.4195 \times 10^{-3}$	
	16	$2.2920 \times 10^{-3}$	2.8377	$1.3514 \times 10^{-3}$	2.4569
	32	$2.8191 \times 10^{-4}$	3.0233	$1.8556 \times 10^{-4}$	2.8645
	64	$3.2609 \times 10^{-5}$	3.1119	$2.2573 \times 10^{-5}$	3.0392
	128	$3.6574 \times 10^{-6}$	3.1564	$2.5937 \times 10^{-6}$	3.1215
	256	$4.0176 \times 10^{-7}$	3.1864	$1.2919 \times 10^{-7}$	3.1721
0.5	8	$3.7940 \times 10^{-3}$		$1.8168 \times 10^{-3}$	
	16	$4.2889 \times 10^{-4}$	3.1451	$2.5900 \times 10^{-4}$	2.8104
	32	$4.3064 \times 10^{-5}$	3.3160	$2.8647 \times 10^{-5}$	3.1765
	64	$4.0768 \times 10^{-6}$	3.4010	$2.8348 \times 10^{-6}$	3.3371
	128	$3.7173 \times 10^{-7}$	3.4551	$2.6407 \times 10^{-7}$	3.4243
	256	$3.0470 \times 10^{-8}$	3.6088	$9.8124 \times 10^{-8}$	3.5948
0.2	8	$5.4498 \times 10^{-4}$		$2.7293 \times 10^{-4}$	
	16	$5.1093 \times 10^{-5}$	3.4150	$3.1455 \times 10^{-5}$	3.1172
	32	$4.2949 \times 10^{-6}$	3.5724	$2.8822 \times 10^{-6}$	3.4480
	64	$3.3828 \times 10^{-7}$	3.6663	$2.3627 \times 10^{-7}$	3.6087
	128	$2.2628 \times 10^{-8}$	3.9020	$1.6173 \times 10^{-8}$	3.8687
	256	$1.8462 \times 10^{-9}$	3.6155	$5.7547 \times 10^{-9}$	3.6574

It is clearly visible from the above Figure 3a,b that scale function  $\zeta(t)$  can stretch or contract the domain.

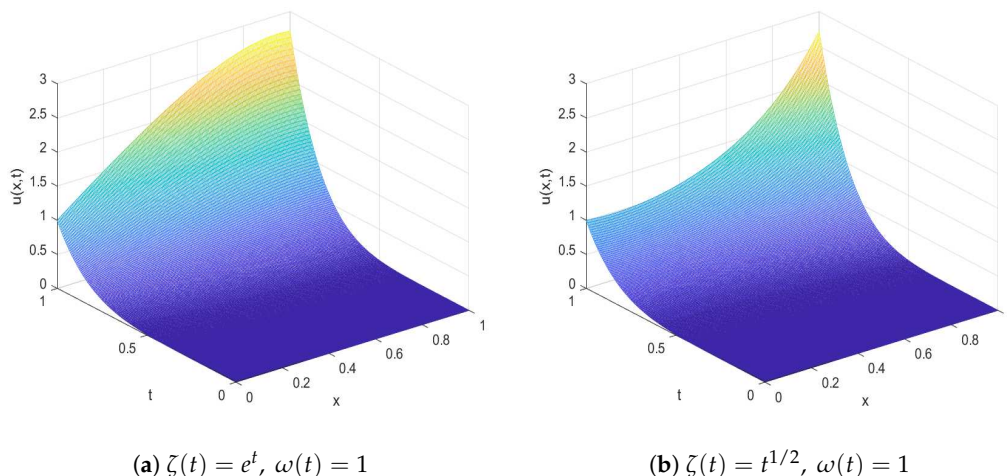


**Figure 3.** Numerical solutions of Example 2 with different choices of weight functions  $\omega(t)$  and scale functions  $\zeta(t)$ , and  $M = N = 200$  with  $\alpha = 0.9$ .

**Table 6.** The maximum errors and convergence rates  $R_x$  for Example 2, when  $\tau = 1/500$  with different  $\alpha$ s.

$M$	$\alpha = 0.2$		$\alpha = 0.5$		$\alpha = 0.8$	
	$E_\infty$ Error	$R_x$	$E_\infty$ Error	$R_x$	$E_\infty$ Error	$R_x$
8	$2.3437 \times 10^{-4}$		$2.1275 \times 10^{-4}$		$1.8078 \times 10^{-4}$	
16	$5.8814 \times 10^{-5}$	1.9945	$5.3334 \times 10^{-5}$	1.9960	$4.5242 \times 10^{-5}$	1.9985
32	$1.4733 \times 10^{-5}$	1.9971	$1.3373 \times 10^{-5}$	1.9958	$1.1319 \times 10^{-5}$	1.9990
64	$3.6832 \times 10^{-6}$	2.0001	$3.3408 \times 10^{-6}$	2.0010	$2.7940 \times 10^{-6}$	2.0183
128	$9.2088 \times 10^{-7}$	1.9999	$8.3276 \times 10^{-7}$	2.0042	$6.6258 \times 10^{-7}$	2.0762

In Table 7, we compare our scheme (37) with Gao et al. ([39], Example 4.1) in temporal direction to fix  $M = 2000$  for particular choices of scale  $\zeta(t) = t$  and weight function  $\omega(t) = 1$ .

**Table 7.** The maximum errors and convergence rates  $R_t$  of Example 4.1 in [39] (page no 43) for different values of  $\alpha$  with  $h = 1/2000$ .

$\alpha$	$N$	Current Scheme		L1–2 [39]	
		$E_\infty$	$R_t$	$E_\infty$	$R_t$
0.9	10	$2.2536 \times 10^{-3}$		$1.8600 \times 10^{-2}$	
	20	$3.2727 \times 10^{-4}$	2.7837	$4.7228 \times 10^{-3}$	1.9776
	40	$4.1906 \times 10^{-5}$	2.9653	$1.1488 \times 10^{-3}$	2.0395
	80	$5.1072 \times 10^{-6}$	3.0366	$2.7367 \times 10^{-4}$	2.0697
	160	$6.1092 \times 10^{-7}$	3.0635	$6.4520 \times 10^{-5}$	2.0846
0.5	10	$2.5470 \times 10^{-4}$		$2.4936 \times 10^{-3}$	
	20	$2.6005 \times 10^{-5}$	3.2919	$4.8366 \times 10^{-4}$	2.3662
	40	$2.4615 \times 10^{-6}$	3.4012	$9.0163 \times 10^{-5}$	2.4234
	80	$2.2827 \times 10^{-7}$	3.4307	$1.6457 \times 10^{-5}$	2.4539
	160	$2.3662 \times 10^{-8}$	3.2701	$2.9700 \times 10^{-6}$	2.4701

**Example 3.** Take the following fractional advection–diffusion equation:

$$\begin{cases} {}_0^C \mathcal{D}_{t, [\zeta(t), \omega(t)]}^\alpha u(x, t) = \frac{\partial^2 u(x, t)}{\partial x^2} - \frac{\partial u(x, t)}{\partial x} + f(x, t), & (x, t) \in (0, 1) \times (0, 1), \\ u(x, 0) = 0, & x \in (0, 1), \\ u(0, t) = 0, \\ u(1, t) = t^7(\sin 1), & t \in (0, 1], \end{cases}$$

where  $f(x, t) = \frac{\Gamma 8}{\Gamma(8-\alpha)} t^{7-\alpha} \sin(x) + t^7(\sin(x) + \cos(x))$ . When  $\zeta(t) = t$  and  $\omega(t) = 1$ , the exact solution is  $u(x, t) = t^7 \sin(x)$ .

To solve this PDE, we use our difference scheme (37). Here, two Tables 8 and 9 are given in support of the numerical results. In Table 8, we take fixed space step size  $h = 1/12000$  and display maximum absolute errors and errors  $E_2$  with respect to norm  $L_2$ , and also the rate of convergence for the temporal direction with different time steps  $N = 8, 16, 32, 64, 128, 256$ . In Table 9, we express maximum errors and convergence order in the space direction to set time steps fixed with  $\tau = 1/500$  and taking different  $M = 8, 16, 32, 64, 128$ .

**Table 8.** Errors  $E_\infty$  and  $E_2$  with convergence rates in time for Example 3, when  $h = 1/12000$  with different  $\alpha$ s.

$\alpha$	$N$	$E_\infty$ Error	$R_t$	$E_2$ Error	$R_t$
0.8	8	$5.2117 \times 10^{-3}$		$4.1672 \times 10^{-1}$	
	16	$7.4158 \times 10^{-4}$	2.8159	$5.9162 \times 10^{-2}$	2.8163
	32	$9.1750 \times 10^{-5}$	3.0148	$7.2113 \times 10^{-3}$	3.0364
	64	$1.0655 \times 10^{-5}$	3.1062	$8.3111 \times 10^{-4}$	3.1171
	128	$1.1991 \times 10^{-6}$	3.1515	$9.3172 \times 10^{-5}$	3.1571
	256	$1.3228 \times 10^{-7}$	3.1803	$1.0259 \times 10^{-5}$	3.1830
0.5	8	$1.5442 \times 10^{-3}$		$1.2679 \times 10^{-1}$	
	16	$1.7157 \times 10^{-4}$	3.1700	$1.3692 \times 10^{-2}$	3.2111
	32	$1.7543 \times 10^{-5}$	3.2898	$1.3792 \times 10^{-3}$	3.3113
	64	$1.6788 \times 10^{-6}$	3.3854	$1.3099 \times 10^{-4}$	3.3964
	128	$1.5678 \times 10^{-7}$	3.4207	$1.2186 \times 10^{-5}$	3.4262
	256	$1.4942 \times 10^{-8}$	3.3913	$1.1596 \times 10^{-6}$	3.3935
0.2	8	$2.8743 \times 10^{-4}$		$2.3613 \times 10^{-2}$	
	16	$2.5557 \times 10^{-5}$	3.4914	$2.0399 \times 10^{-3}$	3.5330
	32	$2.2185 \times 10^{-6}$	3.5261	$1.7445 \times 10^{-4}$	3.5476
	64	$1.7950 \times 10^{-7}$	3.6275	$1.4008 \times 10^{-5}$	3.6385
	128	$1.5668 \times 10^{-8}$	3.5181	$1.2186 \times 10^{-6}$	3.5230
	256	$2.2811 \times 10^{-9}$	2.7800	$1.7738 \times 10^{-7}$	2.7803

**Table 9.** The maximum errors and convergence rates  $R_x$  for Example 3, when  $\tau = 1/500$  with different  $\alpha$ s.

$M$	$\alpha = 0.2$		$\alpha = 0.5$		$\alpha = 0.8$	
	$E_\infty$ Error	$R_x$	$E_\infty$ Error	$R_x$	$E_\infty$ Error	$R_x$
8	$3.0308 \times 10^{-4}$		$2.7311 \times 10^{-4}$		$2.3102 \times 10^{-4}$	
16	$7.6029 \times 10^{-5}$	1.9951	$6.8533 \times 10^{-5}$	1.9946	$5.8003 \times 10^{-5}$	1.9938
32	$1.9050 \times 10^{-5}$	1.9968	$1.7180 \times 10^{-5}$	1.9961	$1.4560 \times 10^{-5}$	1.9941
64	$4.7625 \times 10^{-6}$	2.0000	$4.2962 \times 10^{-6}$	1.9996	$3.6518 \times 10^{-6}$	1.9953
128	$1.1909 \times 10^{-6}$	1.9997	$1.0752 \times 10^{-6}$	1.9985	$9.2444 \times 10^{-7}$	1.9820

In Table 10, we validate the proposed scheme with [21] (Example 5.1). Firstly, we present the max error, the convergence order with fixed  $h = \frac{1}{6000}$  and varying  $N$  with 8, 16, 32, 64, 128 for  $\alpha = 0.368$ . It is noted that the convergence order of our scheme (37) for the temporal direction is almost the same as [21]. After that, we express maximum error and convergence rate for the spatial dimension to set  $\tau = 1/200$  and changing  $M = 4, 8, 16, 32, 64$  for the same value of  $\alpha$ ; we observe that the spatial convergence order of our numerical scheme is same as [21]. Thus, the scheme presented in [21] becomes a particular case of the proposed scheme (37) for  $\zeta(t) = t$  and  $\omega(t) = 1$ . Furthermore, we can compute numerical results for different suitable choices of scale and weight functions.

**Table 10.** The maximum errors and convergence rates  $R_t$  for Example 5.1 in [21], when  $h = 1/6000$ , and spatial convergence rates  $R_x$ , when  $\tau = 1/200$ .

$N$	$\alpha = 0.368$		Cao et al. [21]		$\alpha = 0.368$		Cao et al. [21]	
	$E_\infty$ Error	$R_t$	$R_t$	$M$	$E_\infty$ Error	$R_x$	$R_x$	
8	$8.1539 \times 10^{-4}$			4	$8.8034 \times 10^{-4}$			
16	$7.7720 \times 10^{-5}$	3.3911	3.4031	8	$2.2559 \times 10^{-4}$	1.9643	1.9643	
32	$6.8845 \times 10^{-6}$	3.4969	3.4972	16	$5.6583 \times 10^{-5}$	1.9953	1.9953	
64	$5.8739 \times 10^{-7}$	3.5510	3.5528	32	$1.4173 \times 10^{-5}$	1.9972	1.9972	
128	$4.9904 \times 10^{-8}$	3.5571	3.5836	64	$3.5359 \times 10^{-6}$	2.0030	2.0030	

### 5. Conclusions

A high-order numerical scheme based on cubic interpolation formula is discussed for approximation of GCFD of  $\alpha$ -th order. Properties of discretized coefficients are analyzed and local truncation error in approximation of GCFD is also discussed. Further, we establish a difference scheme for the generalized fractional advection–diffusion equation using the developed approximation formula for GCFD. The stability and convergence of this established scheme to approximate the time fractional generalized advection–diffusion equation are studied. Order of accuracy for the difference scheme is  $\mathcal{O}(\tau^{4-\alpha} + h^2)$ , with step sizes  $\tau$  in time and  $h$  in space directions. The convergence order of the difference scheme is described by some numerical experiments.

Numerical calculations reveal that the proposed difference scheme has  $(4 - \alpha)$ -th order convergence in time; and, in the space direction, it has second-order convergence. The temporal rate of convergence of the scheme for the generalized fractional advection–diffusion equation has the highest accuracy to date. In addition, the developed scheme can be directly used to get other Caputo-type time fractional advection–diffusion equations by selecting suitable scale  $\zeta(t)$  and weight  $\omega(t)$  functions in the generalized Caputo-type fractional derivative. The developed scheme is tested for the cases having smooth solutions of the considered fractional advection–diffusion equation. However, the case of the nonsmooth solutions will be presented in our future works.

**Author Contributions:** Conceptualization, S.K., R.K.P. and R.P.A.; methodology, S.K. and R.K.P.; software, S.K. and R.K.P.; validation, S.K. and R.K.P.; writing—original draft preparation, S.K., R.K.P. and R.P.A.; writing—review and editing, R.K.P. and R.P.A.; supervision, R.K.P.; funding acquisition, R.K.P. and R.P.A. All authors have equally contributed in preparation of the manuscript. All authors have read and agreed to the published version of the manuscript.

**Funding:** This research received no external funding.

**Data Availability Statement:** Not applicable.

**Acknowledgments:** The authors sincerely thank the reviewers for their comments incorporated in the manuscript. The authors are thankful to K. Mustapha, Department of Mathematics and Statistics, King Fahd University of Petroleum and Minerals, Saudi Arabia for his valuable comments incorporated in the manuscript.

**Conflicts of Interest:** The authors declare that they have no known competing financial interests or personal relationships that could have appeared to influence the work reported in this paper.

## References

1. Agrawal, O.P. Some generalized fractional calculus operators and their applications in integral equations. *Fract. Calc. Appl. Anal.* **2012**, *15*, 700–711. [[CrossRef](#)]
2. Benson, D.A.; Wheatcraft, S.W.; Meerschaert, M.M. Application of a fractional advection-dispersion equation. *Water Resour. Res.* **2000**, *36*, 1403–1412. [[CrossRef](#)]
3. Zhou, L.; Selim, H. Application of the fractional advection-dispersion equation in porous media. *Soil Sci. Soc. Am. J.* **2003**, *67*, 1079–1084. [[CrossRef](#)]
4. Baleanu, D.; Wu, G.C.; Zeng, S.D. Chaos analysis and asymptotic stability of generalized Caputo fractional differential equations. *Chaos Solitons Fractals* **2017**, *102*, 99–105. [[CrossRef](#)]
5. Iqbal, M.S.; Yasin, M.W.; Ahmed, N.; Akgül, A.; Rafiq, M.; Raza, A. Numerical simulations of nonlinear stochastic Newell-Whitehead-Segel equation and its measurable properties. *J. Comput. Appl. Math.* **2023**, *418*, 114618. [[CrossRef](#)]
6. Partohaghighi, M.; Mirtalebi, Z.; Akgül, A.; Riaz, M.B. Fractal-fractional Klein-Gordon equation: A numerical study. *Results Phys.* **2022**, *42*, 105970. [[CrossRef](#)]
7. Dan, D.; Mueller, C.; Chen, K.; Glazier, J.A. Solving the advection-diffusion equations in biological contexts using the cellular Potts model. *Phys. Rev. E* **2005**, *72*, 041909. [[CrossRef](#)]
8. Verwer, J.; Blom, J.; Hundsdorfer, W. An implicit-explicit approach for atmospheric transport-chemistry problems. *Appl. Numer. Math.* **1996**, *20*, 191–209. [[CrossRef](#)]
9. Dehghan, M. Weighted finite difference techniques for the one-dimensional advection-diffusion equation. *Appl. Math. Comput.* **2004**, *147*, 307–319. [[CrossRef](#)]
10. Mohebbi, A.; Dehghan, M. High-order compact solution of the one-dimensional heat and advection-diffusion equations. *Appl. Math. Model.* **2010**, *34*, 3071–3084. [[CrossRef](#)]
11. Owolabi, K.M. High-dimensional spatial patterns in fractional reaction-diffusion system arising in biology. *Chaos Solitons Fractals* **2020**, *134*, 109723. [[CrossRef](#)]
12. Podlubny, I. *Fractional Differential Equations: An Introduction to Fractional Derivatives, Fractional Differential Equations, to Methods of Their Solution and Some of Their Applications*; Elsevier: Amsterdam, The Netherlands, 1998.
13. Anatoly, A.K. Hadamard-type fractional calculus. *J. Korean Math. Soc.* **2001**, *38*, 1191–1204.
14. Gaboury, S.; Tremblay, R.; Fugère, B.J. Some relations involving a generalized fractional derivative operator. *J. Inequalities Appl.* **2013**, *2013*, 1–9. [[CrossRef](#)]
15. Atangana, A.; Baleanu, D. New fractional derivatives with nonlocal and non-singular kernel: Theory and application to heat transfer model. *arXiv* **2016**, arXiv:1602.03408.
16. Mustapha, K. An L1 approximation for a fractional reaction-diffusion equation, a second-order error analysis over time-graded meshes. *SIAM J. Numer. Anal.* **2020**, *58*, 1319–1338. [[CrossRef](#)]
17. Alikhanov, A.A. A new difference scheme for the time fractional diffusion equation. *J. Comput. Phys.* **2015**, *280*, 424–438. [[CrossRef](#)]
18. Abu Arqub, O. Numerical solutions for the Robin time-fractional partial differential equations of heat and fluid flows based on the reproducing kernel algorithm. *Int. J. Numer. Methods Heat Fluid Flow* **2018**, *28*, 828–856. [[CrossRef](#)]
19. Li, Z.; Yan, Y. Error estimates of high-order numerical methods for solving time fractional partial differential equations. *Fract. Calc. Appl. Anal.* **2018**, *21*, 746–774. [[CrossRef](#)]
20. Lv, C.; Xu, C. Error analysis of a high order method for time-fractional diffusion equations. *SIAM J. Sci. Comput.* **2016**, *38*, A2699–A2724. [[CrossRef](#)]
21. Cao, J.; Li, C.; Chen, Y. High-order approximation to Caputo derivatives and Caputo-type advection-diffusion Equations (II). *Fract. Calc. Appl. Anal.* **2015**, *18*, 735–761. [[CrossRef](#)]
22. Xu, Y.; Agrawal, O.P. Numerical solutions and analysis of diffusion for new generalized fractional Burgers equation. *Fract. Calc. Appl. Anal.* **2013**, *16*, 709–736. [[CrossRef](#)]
23. Kumar, K.; Pandey, R.K.; Sultana, F. Numerical schemes with convergence for generalized fractional integro-differential equations. *J. Comput. Appl. Math.* **2021**, *388*, 113318. [[CrossRef](#)]
24. Diethelm, K. An efficient parallel algorithm for the numerical solution of fractional differential equations. *Fract. Calc. Appl. Anal.* **2011**, *14*, 475–490. [[CrossRef](#)]
25. Zheng, Y.; Li, C.; Zhao, Z. A note on the finite element method for the space-fractional advection diffusion equation. *Comput. Math. Appl.* **2010**, *59*, 1718–1726. [[CrossRef](#)]
26. Mardani, A.; Hooshmandasl, M.R.; Heydari, M.H.; Cattani, C. A meshless method for solving the time fractional advection-diffusion equation with variable coefficients. *Comput. Math. Appl.* **2018**, *75*, 122–133. [[CrossRef](#)]
27. Li, C.; Cai, M. High-order approximation to Caputo derivatives and Caputo-type advection-diffusion equations: Revisited. *Numer. Funct. Anal. Optim.* **2017**, *38*, 861–890. [[CrossRef](#)]
28. Yadav, S.; Pandey, R.K.; Shukla, A.K.; Kumar, K. High-order approximation for generalized fractional derivative and its application. *Int. J. Numer. Methods Heat Fluid Flow* **2019**, *29*, 3515–3534. [[CrossRef](#)]

29. Tian, W.; Deng, W.; Wu, Y. Polynomial spectral collocation method for space fractional advection–diffusion equation. *Numer. Methods Partial Differ. Equations* **2014**, *30*, 514–535. [[CrossRef](#)]
30. Zhuang, P.; Liu, F.; Anh, V.; Turner, I. Numerical methods for the variable-order fractional advection-diffusion equation with a nonlinear source term. *SIAM J. Numer. Anal.* **2009**, *47*, 1760–1781. [[CrossRef](#)]
31. Singh, D.; Sultana, F.; Pandey, R.K. Approximation of Caputo-Prabhakar derivative with application in solving time fractional Advection-Diffusion equation. *Int. J. Numer. Methods Fluids* **2022**, *94*, 896–919. [[CrossRef](#)]
32. Kannan, R.; Wang, Z.J. LDG2: A variant of the LDG flux formulation for the spectral volume method. *J. Sci. Comput.* **2011**, *46*, 314–328. [[CrossRef](#)]
33. Kannan, R.; Wang, Z.J. A study of viscous flux formulations for a p-multigrid spectral volume Navier Stokes solver. *J. Sci. Comput.* **2009**, *41*, 165–199. [[CrossRef](#)]
34. Kumar, K.; Pandey, R.K.; Sharma, S.; Xu, Y. Numerical scheme with convergence for a generalized time-fractional Telegraph-type equation. *Numer. Methods Partial Differ. Equ.* **2019**, *35*, 1164–1183. [[CrossRef](#)]
35. Cao, W.; Xu, Y.; Zheng, Z. Finite difference/collocation method for a generalized time-fractional KDV equation. *Appl. Sci.* **2018**, *8*, 42. [[CrossRef](#)]
36. Xu, Y.; He, Z.; Agrawal, O.P. Numerical and analytical solutions of new generalized fractional diffusion equation. *Comput. Math. Appl.* **2013**, *66*, 2019–2029. [[CrossRef](#)]
37. Ding, Q.; Wong, P.J. A higher order numerical scheme for generalized fractional diffusion equations. *Int. J. Numer. Methods Fluids* **2020**, *92*, 1866–1889. [[CrossRef](#)]
38. Sultana, F.; Pandey, R.K.; Singh, D.; Agrawal, O.P. High order approximation on non-uniform meshes for generalized time-fractional telegraph equation. *MethodsX* **2022**, *9*, 101905. [[CrossRef](#)] [[PubMed](#)]
39. Gao, G.; Sun, Z.; Zhang, H. A new fractional numerical differentiation formula to approximate the Caputo fractional derivative and its applications. *J. Comput. Phys.* **2014**, *259*, 33–50. [[CrossRef](#)]
40. Xu, Y.; He, Z.; Xu, Q. Numerical solutions of fractional advection–diffusion equations with a kind of new generalized fractional derivative. *Int. J. Comput. Math.* **2014**, *91*, 588–600. [[CrossRef](#)]

**Disclaimer/Publisher’s Note:** The statements, opinions and data contained in all publications are solely those of the individual author(s) and contributor(s) and not of MDPI and/or the editor(s). MDPI and/or the editor(s) disclaim responsibility for any injury to people or property resulting from any ideas, methods, instructions or products referred to in the content.